EUROPEAN ORGANIZATION FOR NUCLEAR RESEARCH (CERN)

CERN-EP-2016-292
2017/10/24

CMS-HIG-16-015

Search for light bosons in decays of the 125 GeV Higgs boson in proton-proton collisions at $\sqrt{s} = 8$ TeV

The CMS Collaboration*

Abstract

A search is presented for decays beyond the standard model of the 125 GeV Higgs bosons to a pair of light bosons, based on models with extended scalar sectors. Light boson masses between 5 and 62.5 GeV are probed in final states containing four τ leptons, two muons and two b quarks, or two muons and two τ leptons. The results are from data in proton-proton collisions corresponding to an integrated luminosity of 19.7 fb^{-1}, accumulated by the CMS experiment at the LHC at a center-of-mass energy of 8 TeV. No evidence for such exotic decays is found in the data. Upper limits are set on the product of the cross section and branching fraction for several signal processes. The results are also compared to predictions of two-Higgs-doublet models, including those with an additional scalar singlet.

Published in the Journal of High Energy Physics as doi:10.1007/JHEP10(2017)076.

*See Appendix A for the list of collaboration members

1 Introduction

Studies of the recently discovered spin-0 particle h [1–3], with a mass of 125 GeV and with properties consistent with the standard model (SM) Higgs boson [4], severely constrain SM extensions that incorporate scalar sectors [5–7]. There are many well-motivated models that predict the existence of decays of the Higgs boson to non-SM particles [8]. Without making assumptions about the h(125) couplings to quarks, leptons, and vector bosons, other than that the scalar sector is composed only of doublets and singlets, the ATLAS and CMS collaborations at the CERN LHC exclude at a 95% confidence level (CL) branching fractions of the Higgs boson to beyond SM (BSM) particles, $\mathcal{B}(\mathrm{h} \to \mathrm{BSM})$, greater than 49% and 52%, respectively [5, 6]. Branching fractions as low as 34% can be excluded at 95% CL by combining the results obtained by the two experiments [4, 9]. The LHC experiments are expected to be able to constrain branching fractions to new particles beyond the 5-10% level using indirect measurements [10–12]. In this context, it is interesting to explore the possibility of decays of the SM-like Higgs particle to lighter scalars or pseudoscalars [8, 13–15].

The SM Higgs boson has an extremely narrow width relative to its mass, because of its exceedingly small Yukawa couplings to the SM fermions it can decay to. This suggests that any non-SM final state is likely to have a larger partial width, and therefore a non-negligible branching fraction, compared to decays to SM particles [8]. Examples of BSM models that provide such additional decay modes include those in which the Higgs boson serves as a portal to hidden-sector particles (e.g. dark matter) that can couple to SM gauge bosons and fermions [16]. Other models have extended scalar sectors, such as those proposed in two-Higgs-doublet models (2HDM) [17–21], in the next-to-minimal supersymmetric model (NMSSM) [22, 23], or in other models in which a singlet Higgs field is added to the SM doublet sector. The NMSSM is particularly well motivated as it provides a solution to the μ problem associated with supersymmetry breaking, and can provide a contribution to electroweak baryogenesis [24, 25].

Both 2HDM and NMSSM may contain a light enough pseudoscalar state (a), which can yield a large $\mathrm{h} \to \mathrm{aa}$ branching fraction. In 2HDM, the mass of the pseudoscalar boson a is a free parameter, but, if $m_\mathrm{a} < m_\mathrm{h}/2$, fine-tuning of the 2HDM potential is required to keep the branching fraction $\mathcal{B}(\mathrm{h} \to \mathrm{aa})$ consistent with LHC data [26]. In NMSSM, there are two pseudoscalar Higgs bosons, a_1 and a_2. Constraints from the Peccei–Quinn [27, 28] and R [23, 29] symmetries imply that the lighter a_1 is likely to have a mass smaller than that of the h boson [25], and, since it is typically a singlet, suppression of $\mathcal{B}(\mathrm{h} \to \mathrm{a}_1\mathrm{a}_1)$ to a level compatible with observations is a natural possibility. The minimal supersymmetric model (MSSM) contains a single pseudoscalar (A), but the structure of the MSSM Higgs potential is such that its mass cannot be below about 95 GeV when the scalar (to be identified with h) has mass close to 125 GeV and is SM-like as implied by the LHC data [30]. The phenomenology of decays of the observed SM-like Higgs boson to a pair of lighter Higgs bosons is detailed in Refs. [8, 31–38] for 2HDM, in Refs. [8, 39–42] in the context of NMSSM or NMSSM-like, and in Refs. [8, 43, 44] in the general case of adding a singlet field to the SM or to a 2HDM prescription.

The 2HDM contains two Higgs doublet fields, Φ_1 and Φ_2, which, after symmetry breaking, lead to five physical states. One of the free parameters in the 2HDM is $\tan\beta$, the ratio between the vacuum expectation values for the two doublets, expressed as $\tan\beta = v_2/v_1$. The lightest scalar of the 2HDM is compatible with the SM-like properties of the discovered boson in the limit where the other scalars all have large masses (decoupling limit), and also in the alignment limit [45], in which the neutral Higgs boson mass eigenstate is approximately aligned with the direction of the vacuum expectation values for the scalar field. Approximate alignment, which is sufficient for consistency with LHC data, is possible for a large portion of parameter

space [45], particularly when the pseudoscalar boson has sufficiently small mass to make $h \to aa$ decays possible.

At lowest order, there are four types of 2HDM without flavor-changing neutral currents (FCNC), which can be characterized through the coupling of each fermion to the doublet structure, as shown in Table 1. The ratios of the Yukawa couplings of the pseudoscalar boson of the 2HDM relative to those of the Higgs boson of the SM are functions of $\tan\beta$ and of the type of 2HDM, and are given in Table 2. Type-1 and type-2 models are the ones commonly considered, and the latter are required in supersymmetric models. In these two cases, the leptons have the same couplings as the down-type quarks. In type-3 2HDM, all quarks couple to Φ_2 and all leptons couple to Φ_1, with the result that all leptonic or quark couplings of the pseudoscalar a are proportional to $\tan\beta$ or $\cot\beta$, so that for large $\tan\beta$ the leptonic decays of a dominate.

As implied previously, a complex $\mathrm{SU}(2)_\mathrm{L}$ singlet field S can be added to 2HDM; such models are called 2HDM+S, and include the NMSSM as a special case. If S mixes only weakly with the doublets, one of the CP-even scalars can again have SM-like properties. The addition of the singlet S leads to two additional singlet states, a second CP-odd scalar and a third CP-even scalar, which inherit a mixture of the fermion interactions of the Higgs doublets. After mixing among the spin-0 states, the result is two CP-odd scalars, a_1 and a_2, and three CP-even scalars, h_1, h_2, and h_3. Of the latter, one can be identified with the observed SM-like state, h. The branching fraction of the h boson to a pair of CP-even or CP-odd bosons can be sizeable, leading to a wide variety of possible exotic h decays. In the 2HDM and its extensions, the ratio

Table 1: Doublets to which the different types of fermions couple in the four types of 2HDM without FCNC at lowest order.

	Type-1	Type-2	Type-3 (lepton-specific)	Type-4 (flipped)
Up-type quarks	Φ_2	Φ_2	Φ_2	Φ_2
Down-type quarks	Φ_2	Φ_1	Φ_2	Φ_1
Charged leptons	Φ_2	Φ_1	Φ_1	Φ_2

Table 2: Ratio of the Yukawa couplings of the pseudoscalar boson a of the 2HDM relative to those of the Higgs boson of the SM, in the four types of 2HDM without FCNC at lowest order.

	Type-1	Type-2	Type-3 (lepton-specific)	Type-4 (flipped)
Up-type quarks	$\cot\beta$	$\cot\beta$	$\cot\beta$	$\cot\beta$
Down-type quarks	$-\cot\beta$	$\tan\beta$	$-\cot\beta$	$\tan\beta$
Charged leptons	$-\cot\beta$	$\tan\beta$	$\tan\beta$	$-\cot\beta$

of the decay widths of a pseudoscalar boson to different types of leptons depends only on the masses of these leptons. In particular, for decays into muons and τ leptons, and a pseudoscalar boson of mass m_a, we can write [8, 46]:

$$\frac{\Gamma(\mathrm{a} \to \mu^+\mu^-)}{\Gamma(\mathrm{a} \to \tau^+\tau^-)} = \frac{m_\mu^2\sqrt{1-(2m_\mu/m_\mathrm{a})^2}}{m_\tau^2\sqrt{1-(2m_\tau/m_\mathrm{a})^2}}. \tag{1}$$

This kind of relation can also be written for electrons and muons. In models where the pseudoscalar boson a decays only to leptons, its branching fraction to τ leptons is greater than 99% for pseudoscalar boson masses above 5 GeV. This is a good approximation for pseudoscalar

masses below twice the bottom quark mass, or for type-3 2HDM, assuming loop-induced decays such as $a \to gg$ are ignored. In type-1 and -2, and their extensions, a similar relation exists between the partial decay widths of the pseudoscalar boson to leptons and to down-type quarks, for example, for muons and b quarks, we can write [8, 46]:

$$\frac{\Gamma(a \to \mu^+\mu^-)}{\Gamma(a \to b\bar{b})} = \frac{m_\mu^2\sqrt{1-(2m_\mu/m_a)^2}}{3m_b^2\sqrt{1-(2m_b/m_a)^2}\,(1+\text{QCD corrections})}. \quad (2)$$

The factor of three in the denominator reflects the number of b quark colors, and perturbative quantum chromodynamic (QCD) corrections are typically $\simeq$20% [8]. In models of type-3 or -4, however, the ratio of the partial decay widths depends on $\tan\beta$.

Three searches for decays of the 125 GeV Higgs boson to pairs of lighter scalars or pseudoscalars are described in this paper, where, for notational simplicity, the symbol a refers to both the light scalar and light pseudoscalar:

- $h \to aa \to 4\tau$,
- $h \to aa \to 2\mu 2b$,
- $h \to aa \to 2\mu 2\tau$.

The first analysis focuses on light boson masses above twice the τ mass, using dedicated techniques to reconstruct the Lorentz-boosted τ lepton pairs. The two other analyses focus on masses large enough that the decay products are well separated from each other, and below half of the Higgs boson mass. The production of the Higgs boson is assumed to be SM-like. The results of these searches are interpreted in the 2HDM and 2HDM+S contexts, together with the two other analyses described in greater detail in the references given below:

- $h \to aa \to 4\mu$ [47];
- $h \to aa \to 4\tau$, using a different boosted τ lepton reconstruction technique than the analysis with the same final state listed above [48].

These analyses are based on proton-proton collision data corresponding to an integrated luminosity of 19.7 fb^{-1}, recorded by the CMS experiment at the LHC at a center-of-mass energy of 8 TeV. The D0 Collaboration at the Fermilab Tevatron published results for $h \to aa \to 2\mu 2\tau$ and $h \to aa \to 4\mu$ searches for pseudoscalar masses m_a between 3.5 and 19 GeV [49], while ATLAS reported a search for $h \to aa \to 2\mu 2\tau$ decays with m_a between 3.7 and 50 GeV, using special techniques to reconstruct Lorentz-boosted τ lepton pairs [50]. Additionally, CMS performed searches for direct production of light pseudoscalars with mass between 5.5 and 14 GeV that decay to pairs of muons [51], and with mass between 25 and 80 GeV that decay to pairs of τ leptons [52].

2 The CMS detector, event simulation, and reconstruction

The central feature of the CMS apparatus is a superconducting solenoid of 6 m internal diameter, providing an axial magnetic field of 3.8 T. Within the solenoid volume are a silicon pixel and strip tracker, a lead tungstate crystal electromagnetic calorimeter (ECAL), and a brass and scintillator hadron calorimeter (HCAL), each composed of a barrel and two endcap sections. Extensive forward calorimetry complements the coverage provided by the barrel and endcap detectors. Muons are detected in gas-ionization chambers embedded in the steel flux-return yoke outside the solenoid.

The first level of the CMS trigger system, composed of specialized hardware processors, uses information from the calorimeters and muon detectors to select the most interesting events in a fixed time interval of less than 4 μs. The high-level trigger processor farm further decreases the event rate from around 100 kHz to less than 1 kHz, before data storage. A detailed description of the CMS detector, together with a definition of the coordinate system used and the relevant kinematic variables, can be found in Ref. [53].

Samples of simulated events are used to model signal and background processes. Drell-Yan, W+jets, $\mathrm{t\bar{t}}$, and diboson events are simulated with MADGRAPH 5.1.3.30 [54] using the matrix element calculation at leading-order (LO) precision in QCD; PYTHIA 6.426 [55] is used for parton showering, hadronization, and most particle decays; and TAUOLA 27.121.5 [56] is used specifically for τ lepton decays. Single top quark events produced in association with a W boson are generated using POWHEG 1.0 r1380 [57–60], interfaced to PYTHIA for parton showering. Signal samples are generated with PYTHIA using its built-in 2HDM and NMSSM generator routines. Background and signal samples use the CTEQ6L [61] parton distribution functions (PDFs). Minimum-bias collision events generated with PYTHIA are added to all Monte Carlo (MC) samples to reproduce the observed concurrent pp collisions in each bunch crossing (pileup). The average number of pileup interactions in 2012 data was 20. All generated events are passed through the full GEANT4 [62, 63] based simulation of the CMS apparatus and are reconstructed with the same CMS software that is used to reconstruct the data.

Event reconstruction relies on a particle-flow (PF) algorithm, which combines information from different subdetectors to reconstruct individual particles [64, 65]: neutral and charged hadrons, photons, electrons, and muons. More complex objects are reconstructed by combining the PF candidates. A deterministic annealing algorithm [66, 67] is used to reconstruct the collision vertices. The vertex with the maximum sum in the squared transverse momenta (p_{T}^2) of all associated charged particles is defined as the primary vertex. The longitudinal and radial distances of the vertex from the center of the detector must be smaller than 24 and 2 cm, respectively.

Muons are reconstructed by matching hits in the silicon tracker and in the muon system [68]. Global muon tracks are fitted from hits in both detectors. A preselection is applied to the global muon tracks, with requirements on their impact parameters, to suppress non-prompt muons produced from the pp collision or muons from cosmic rays.

Electrons are reconstructed from groups of one or more associated clusters of energy deposited in the ECAL. Electrons are identified through a multivariate (MVA) method [69] trained to discriminate electrons from quark and gluon jets [70].

The muon and electron relative isolation is defined as:

$$I_{\mathrm{rel}} = \left[\sum_{\mathrm{charged}} p_{\mathrm{T}} + \max\left(0, \sum_{\mathrm{neutral}} p_{\mathrm{T}} + \sum_{\gamma} p_{\mathrm{T}} - \frac{1}{2} \sum_{\mathrm{charged,PU}} p_{\mathrm{T}}\right)\right] / p_{\mathrm{T}}, \tag{3}$$

where $\Sigma_{\mathrm{charged}} p_{\mathrm{T}}$ is the sum of the magnitudes of the transverse momenta of charged hadrons, electrons and muons originating from the primary vertex, $\Sigma_{\mathrm{neutral}} p_{\mathrm{T}}$ is the corresponding sum for neutral hadrons and Σ_{γ} for photons, and $\Sigma_{\mathrm{charged,PU}} p_{\mathrm{T}}$ is the sum of the transverse momentum of charged hadrons, electrons, and muons originating from other reconstructed vertices. The particles considered in the isolation calculation are inside a cone with a radius $\Delta R = \sqrt{(\Delta\eta)^2 + (\Delta\phi)^2} = 0.4$ around the lepton direction, where $\Delta\eta$ and $\Delta\phi$ are the differences of pseudorapidity and azimuthal angle in radians between the particles and the lepton direction, respectively. The factor $\frac{1}{2}$ originates from the approximate ratio of the neutral to charged candidates in a jet. In the search for $\mathrm{h} \to \mathrm{aa} \to 4\tau$, the isolation criteria are extended to veto the presence of reconstructed leptons within the $\Delta R = 0.4$ cone, as detailed in Section 3.

Jets are reconstructed by clustering charged and neutral particles using an anti-k_T algorithm [71], implemented in the FASTJET library [72, 73], with a distance parameter of 0.5. The reconstructed jet energy is corrected for effects from the detector response as a function of the jet p_T and η. Furthermore, contamination from pileup, underlying events, and electronic noise is subtracted on a statistical basis [74]. An eta-dependent tuning of the jet energy resolution in the simulation is performed to match the resolution observed in data [74]. The combined secondary vertex (CSV) algorithm is used to identify jets that are likely to originate from a b quark ("b jets"). The algorithm exploits the track-based lifetime information together with the secondary vertices associated with the jet to provide a likelihood ratio discriminator for the b jet identification [75]. A set of p_T-dependent correction factors are applied to simulated events to account for differences in the b tagging efficiency between data and simulation [75].

Tau leptons that decay into a jet of hadrons and a neutrino, denoted τ_h, are identified with a hadron-plus-strips (HPS) algorithm, which matches tracks and ECAL energy deposits to reconstruct τ candidates in one of the one-prong, one-prong + π^0(s), and three-prong decay modes [76]. Reconstructed τ_h candidates are seeded from anti-k_T jets with a distance parameter of 0.5. For each jet, τ candidates are constructed from the jet constituents according to criteria that include consistency with the vertex of the hard interaction and consistency with the π^0 mass hypothesis. Two methods for rejecting quark and gluon jets are employed, depending on the analysis. The first is a straightforward selection based on the isolation variable, while the second uses a multivariate analysis (MVA) discriminator that takes into account variables related to the isolation, to the transverse impact parameter of the leading track of the τ_h candidate, and to the distance between the τ production point and the decay vertex in the case of three-prong decay modes [76]. MVA-based discriminators are implemented to reduce the rates at which electrons or muons are misidentified as τ_h candidates. Muons or electrons from leptonic decays of τ leptons are indistinguishable from prompt leptonic decay products of W and Z bosons and are reconstructed as described earlier.

The missing transverse energy, E_T^{miss}, is defined as the magnitude of $\vec{p}_T^{miss}$, which is the negative sum of $\vec{p}_T$ of all PF candidates. The jet energy calibration introduces corrections to the E_T^{miss} measurement. The E_T^{miss} significance variable, which estimates the compatibility of the reconstructed E_T^{miss} with zero, is calculated via a likelihood function on an event-by-event basis [77].

As part of the quality requirements, events in which an abnormally high level of noise is detected in the HCAL barrel or endcap detectors are rejected [78].

3 Search for $h \to aa \to 4\tau$ decays

This analysis considers 4τ final states arising from $h \to aa \to 4\tau$ decay, where the Higgs boson is produced via gluon fusion (ggh), in association with a W or Z boson (Wh or Zh), or via vector boson fusion (VBF). Light boson masses are probed in the range $5-15$ GeV, where the branching fraction of the light boson to τ leptons is expected to be large in certain 2HDM models. To illustrate the performance of the analysis, a mass of 9 GeV is chosen as a benchmark model throughout this section; it represents a type-2 2HDM variant in which the pseudoscalar branching fraction to τ leptons is dominant. The large Lorentz boost of the a boson at such light masses causes its decay products to overlap. To maximize the sensitivity to overlapping τ leptons, a special boosted $\tau\tau$ pair reconstruction technique is employed, based on the specific final state in which one τ lepton decays to a muon. This analysis is performed in two search regions based on the transverse mass (m_T) formed from a high-p_T muon and the p_T^{miss}. These two regions are designed to distinguish between the Wh production mode and other modes (primarily ggh) without significant E_T^{miss}.

3.1 Event selection

Events considered in this search are selected with a single muon trigger that requires the presence of an isolated muon with $p_T > 24\,\text{GeV}$ and $|\eta| < 2.1$. This analysis specifically targets the event topology with one isolated high p_T muon, and at least one boosted $\tau\tau$ pair in which one τ lepton decays to a muon and neutrinos (τ_μ). No assumption is made on the decay of the second τ lepton in the boosted $\tau\tau$ pair. Because of the features of this topology, it is convenient to define the "trigger muon" candidate, μ_{trg}, referring to the isolated high p_T muon triggering the event, and the "$\tau_\mu\tau_X$ object", aiming to reconstruct the decay products of the boosted $\tau\tau$ pair. This topology is characteristic of two classes of signal events:

1. The Higgs boson is produced through gluon fusion or vector boson fusion and decays as $h \to a(\to \tau_\mu\tau_X)a(\to \tau_\mu\tau_X)$. When the τ_μ from the decay of one a has both a high p_T and is well separated from the τ_X arising from the same decay, it will satisfy the trigger muon criteria. The other $\tau\tau$ pair is reconstructed as a $\tau_\mu\tau_X$ object.
2. The Higgs boson is produced through associated production with a W or a Z boson that then decays to isolated muons. The Higgs boson decay considered here is $h \to a(\to \tau_\mu\tau_X)a(\to \tau_X\tau_X)$. The muon from the W or Z decay is required to pass the trigger criteria, one of the $\tau\tau$ pairs is reconstructed as a $\tau_\mu\tau_X$ object, and no requirement is applied to the second $\tau\tau$ pair.

The remainder of this subsection describes selection and reconstruction criteria for the muon that fires the trigger, and for the $\tau_\mu\tau_X$ object.

The reconstructed μ_{trg} object must be located within $\Delta R < 0.1$ of the isolated muon reconstructed in the trigger system. It is also required to have $p_T > 25\,\text{GeV}$, $|\eta| < 2.1$, be well reconstructed in both the muon detectors and the silicon tracker, have a high-quality track fit, and be consistent with originating from the primary pp interaction in the event. In addition, it must be isolated from other photons, hadrons, and leptons in the detector. Isolation from photons and hadrons is enforced by requiring that the muon relative isolation, as defined in Eq. (3), is less than 0.12. To be isolated from other leptons, the trigger muon is required to have no identified electrons ($p_T > 7\,\text{GeV}$, $|\eta| < 2.5$), muons ($p_T > 5\,\text{GeV}$, $|\eta| < 2.4$, passing τ_μ criteria below), or τ leptons ($p_T > 10\,\text{GeV}$, $|\eta| < 2.3$, passing modified HPS criteria, as described below) reconstructed within $\Delta R = 0.4$ of the trigger muon direction. The requirement of isolation from nearby leptons, in addition to the isolation requirement of Eq. (3), ensures that a trigger muon originating from a τ lepton decay, where the τ lepton originates from a pseudoscalar decay, is well isolated from the other τ lepton in the pseudoscalar decay pair. In this way, the high level trigger and "trigger muon" identification criteria are efficient for low-p_T τ decay muons expected to pass the trigger in the ggh and VBF production modes, provided that τ leptons from the pseudoscalar decay are well separated or one of the τ leptons has p_T low enough not to affect the isolation of the other τ lepton. The isolation requirements are also efficient for high-p_T isolated muons from W boson decays expected in the Wh associated production mode.

The muon from the τ lepton decaying via the muon channel (τ_μ) is required to have $p_T > 5\,\text{GeV}$ and $|\eta| < 2.4$, be well reconstructed in the silicon tracker, have a high-quality track fit, be consistent with originating from the primary vertex in the event, and be separated by at least $\Delta R = 0.5$ from the trigger muon. Because no isolation requirement is placed on the τ_μ candidate, it can be identified with high efficiency in the presence of a nearby τ lepton. Overall, the trigger and τ_μ quality criteria are similar, but the τ_μ criteria are optimized for low-p_T non-isolated muons, while the trigger muon criteria are optimized for high-p_T isolated muons.

Since the final state in this analysis includes a pair of boosted τ leptons from pseudoscalar decay, the HPS algorithm is modified to maintain high efficiency for overlapping τ leptons. All jet constituents are checked for the presence of τ_μ candidates as defined above. Only jets that have at least one muon candidate passing the τ_μ criteria among their constituents are used to seed the HPS reconstruction. Within these selected jets, the muon is excluded from the set of jet constituents before running the HPS reconstruction algorithm. The HPS reconstruction then proceeds as described in Section 2, and the resulting τ lepton is required to have $p_T > 20\,\text{GeV}$ and $|\eta| < 2.3$. The combination of the τ_μ and isolated HPS τ candidates resulting from this selection form the $\tau_\mu\tau_X$ object as it is designed to reconstruct boosted $a \to \tau_\mu\tau_X$ decays. The HPS τ candidate is referred to as τ_X because no anti-electron or anti-muon discriminators are applied to it; although τ leptons decaying to electrons and muons can thus pass the HPS selection, the vast majority ($\simeq$97%) of selected τ candidates in simulated $h \to aa$ samples are hadronically decaying τ leptons. The modified HPS τ lepton reconstruction and isolation requirements have a similar efficiency for $h \to aa$ decays as the standard HPS and isolation requirements have for $Z \to \tau\tau$ decays.

This analysis requires at least one $\tau_\mu\tau_X$ object, which reconstructs a single $a \to \tau\tau$ decay, per event. The $\tau_\mu\tau_X$ object consists of a muon, one or three other charged particle tracks, and zero or more neutral hadrons, and could therefore arise from misidentifying the decay products of a bottom quark jet. To further distinguish $\tau_\mu\tau_X$ objects from background, the seed jet of the HPS reconstructed τ_X (excluding any identified τ_μ candidate) is required not to be identified as a b jet.

3.2 Signal and background estimation

The main background contributions to this search arise from Drell-Yan dimuon pairs produced in association with jets, ($W \to \mu\nu$) + jets, $t\bar{t}$ with muons in the final state, and QCD multi-jet events. In order to reduce the Drell-Yan background, the trigger muon and τ_X candidates are required to have the same sign (SS) of electric charge. To minimize backgrounds with jets misidentified as τ candidates, the τ_μ and τ_X objects are required to have opposite sign. The signal region is defined by events passing all the requirements described above, as well as $m_{\mu+X} \geq 4\,\text{GeV}$, where $m_{\mu+X}$ is the invariant mass calculated from the four-vectors of the two components of the $\tau_\mu\tau_X$ object. The choice of 4 GeV reduces the expected background contribution by about 95%, while keeping approximately 75% of the expected events in the case of the ggh benchmark 9 GeV pseudoscalar mass sample. Signal acceptance is calculated from the simulated samples for masses between 5 and 15 GeV. The expected signal acceptance is corrected using p_T- and $|\eta|$-dependent scale factors to account for known differences in the b veto efficiency between data and simulation [75].

Events are classified into two analysis bins depending on the value of the transverse mass between the trigger muon momentum and the $\vec{p}_T^{\,\text{miss}}$, defined as

$$m_T = \sqrt{2p_T^{\mu_{trg}} E_T^{\text{miss}} [1 - \cos\Delta\phi(\mu_{trg}, \vec{p}_T^{\,\text{miss}})]}, \tag{4}$$

where $\Delta\phi(\mu_{trg}, \vec{p}_T^{\,\text{miss}})$ is the azimuthal angle between the trigger muon position vector and $\vec{p}_T^{\,\text{miss}}$ vector. The contribution of signal events for the different production modes in the low-m_T and high-m_T bins for a representative pseudoscalar mass of 9 GeV, and assuming $\mathcal{B}(h \to aa)\,\mathcal{B}^2(a \to \tau^+\tau^-) = 0.1$, is given in Table 3. For $m_T \leq 50\,\text{GeV}$, ggh fusion production accounts for about 85% of the expected signal, VBF accounts for another 10%, and associated production accounts for the rest. For $m_T > 50\,\text{GeV}$, ggh and Wh productions each account for about 40% of the expected signal and Zh and VBF productions account for the rest. Dividing selected events

Table 3: Expected signal yields for the $h \to aa \to 4\tau$ process for a representative pseudoscalar mass of 9 GeV, in both m_T bins, assuming SM cross sections and $\mathcal{B}(h \to aa)\,\mathcal{B}^2(a \to \tau^+\tau^-) = 0.1$, in the context of the $h \to aa \to 4\tau$ search. Expected background yields as well as observed numbers of events are also quoted. Only the statistical uncertainty is given for signal yields.

	$m_T \leq 50\,\text{GeV}$	$m_T > 50\,\text{GeV}$
ggh	4.6 ± 0.3	0.8 ± 0.1
Wh	0.27 ± 0.02	0.70 ± 0.03
Zh	0.068 ± 0.005	0.19 ± 0.01
VBF	0.51 ± 0.03	0.09 ± 0.01
SM background	$5.4 \pm 1.0\,(\text{stat})^{+4.2}_{-4.6}\,(\text{syst})$	$6.1 \pm 1.6\,(\text{stat})^{+3.7}_{-3.6}\,(\text{syst})$
Observed	7	14

in two m_T categories increases the sensitivity to models (for example Ref. [79]) where the ggh production rate would be modified with respect to the SM expectation because of different Yukawa couplings of the fermions appearing in the loop, whereas the Wh and Zh production rates would be similar as in the SM in the case of the alignment limit of 2HDM.

There are several mechanisms that result in $\tau_\mu\tau_X$ misidentification, for example jets with semileptonic decays, jets with double semileptonic decays, or resonances in b or light-flavor jet fragmentation. It is impractical to simulate all backgrounds to the required statistical precision. Therefore, the number of background events in the low-m_T (high-m_T) signal region, denoted $N_{\text{bkg}}^{\text{low-}m_T\,(\text{high-}m_T)}(m_{\mu+X} \geq 4\,\text{GeV})$, is estimated independently from three event samples. In each background estimation sample, the isolation energy around the τ_X candidate is required to be between 1 and 5 GeV, as opposed to the signal sample requirement of isolation energy less than 1 GeV. The three samples are:

1. Observed events passing all other signal selections;
2. Simulated Drell-Yan, W+jets, $t\bar{t}$, and diboson events passing all other signal selections;
3. Observed events passing all other signal selections, but with inverted μ_{trg} relative isolation.

The background estimate from each sample is normalized to match the observed data yield in the signal-free region with $m_{\mu+X} < 2\,\text{GeV}$. The final background prediction in the low-m_T (high-m_T) bin is taken as the arithmetic mean of the estimates from the three background estimation samples with $m_T \leq 50\,\text{GeV}$ ($m_T > 50\,\text{GeV}$). The positive (negative) systematic uncertainty is taken as the difference between the largest (smallest) of the three plus (minus) its statistical uncertainty and the average. In the low-m_T bin, the background yield is estimated to be $5.4 \pm 1.0\,(\text{stat})^{+4.2}_{-4.6}\,(\text{syst})$ events, while in the high-m_T bin it is estimated to be $6.1 \pm 1.6\,(\text{stat})^{+3.7}_{-3.6}\,(\text{syst})$ events. The uncertainty on the background yield is dominated by the limited statistical precision in the control samples, owing to the rare final state being probed. This uncertainty is the dominant source of systematic error in the interpretation of the results of this search in terms of an upper limit on the branching fraction of the Higgs boson to light pseudoscalar states.

The relaxed τ_X isolation requirement common to each sample implies that these background estimation samples should be enriched in events with jets. Simulated samples of W+jets and

$\bar{\text{t}}\text{t}$ events, in which the $\tau_\mu\tau_\text{X}$ candidate arises from misidentified jets, have been used to check that events with nonisolated τ_X candidates have the same kinematic properties as those of the signal sample.

Figure 1 shows the estimated misidentified jet background, the search region data, and simulations of the four signal production models for both m_T bins. Seven and fourteen events are observed in the low- and high-m_T bins, respectively.

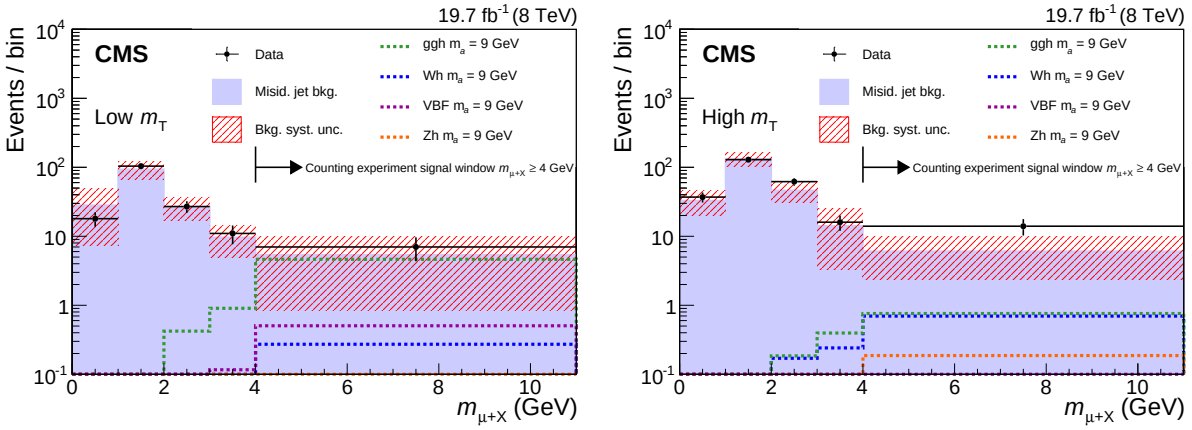

Figure 1: Comparison, for the $\text{h} \to \text{aa} \to 4\tau$ search, of $m_{\mu+\text{X}}$ distributions for data (black markers) and the misidentified jet background estimate (solid histogram) in the low-m_T (left) and high-m_T (right) bins. Predicted signal distributions (dotted lines) for each of the four Higgs boson production mechanisms are also shown; the distributions are normalized to an integrated luminosity of the data sample of 19.7 fb^{-1}, assuming SM Higgs boson production cross sections and $\mathcal{B}(\text{h} \to \text{aa})\,\mathcal{B}^2(\text{a} \to \tau^+\tau^-) = 0.1$. The last bin on the right contains all the events with $m_{\mu+\text{X}} \geq 4$ GeV, which correspond to the numbers reported in Table 3.

4 Search for $\text{h} \to \text{aa} \to 2\mu 2\text{b}$ decays

The search for a new scalar in $\text{h} \to \text{aa} \to 2\mu 2\text{b}$ decays is restricted to masses between 25 and 62.5 GeV. The upper bound is imposed by the kinematic constraint of $m_\text{h} = 125$ GeV, while there is a sensitivity loss for this search below the lower bound due to overlap between the two b jets or the two muons arising from an increased boost of the pseudoscalars [80]. A slightly wider pseudoscalar mass range is however used for the selection, the optimization aiming at maximum expected signal significance, and the eventual background modeling. In particular, the wider mass range ensures a good description of the background distribution over the entire search region, including regions near the boundaries. Events with an invariant mass $m_{\mu\mu}$ outside the range 20-70 GeV are discarded.

4.1 Event selection

In the search for $\text{h} \to \text{aa} \to 2\mu 2\text{b}$ decays, events are triggered based on the presence of two muons with $p_\text{T} > 17$ GeV and $p_\text{T} > 8$ GeV. For the offline selection, the leading muon p_T threshold is increased to 24 GeV, while the subleading muon p_T must exceed 9 GeV. The two muon candidates are required to have opposite electric charges and to be isolated. If more than one muon is found for a given sign, the one with the highest p_T is selected. At least two jets with $p_\text{T} > 15$ GeV and $|\eta| < 2.4$ are required to satisfy b-tag requirements that allow only $\mathcal{O}(1\%)$ of the light quark jets to survive, for an efficiency of $\simeq$65% for genuine b jets. The E_T^miss

significance of the event has to be less than 6. Events outside the $|m_{\mu\mu bb} - 125\,\text{GeV}| < 25\,\text{GeV}$ window are discarded.

4.2 Signal and background estimation

As presented in Table 4, the expected background yield estimated from simulation over the whole mass range considered is 235 ± 35 events, dominated by Drell-Yan events in the dilepton final state, followed by $t\bar{t}$ in dilepton decays, $t\bar{t}\,(\ell\ell)$. This should be compared with 252 events observed in data. To evaluate the signal yield, only the gluon fusion Higgs boson production mechanism with the next-to-leading-order (NLO) cross section of $\sigma_{ggh} \simeq 19.3\,\text{pb}$ [81] is considered. Other SM Higgs production modes are found to contribute less than 5% to the signal yield and are neglected. Assuming a branching fraction of 10% for $h \to aa$ together with $\tan\beta = 2$ in the context of type-3 2HDM+S, one can obtain $2\mathcal{B}(a \to b\bar{b})\mathcal{B}(a \to \mu^+\mu^-) = 1.7 \times 10^{-3}$ for $m_a = 30\,\text{GeV}$, where no strong dependence on m_a is expected for $\mathcal{B}(a \to f\bar{f})$, with f being a muon or a b quark [8]. In this scenario, about one signal event is expected to survive the event selection discussed earlier.

Table 4: Expected signal and background yields, together with the number of observed events, for the $h \to aa \to 2\mu 2b$ search, in the range $20 \leq m_{\mu\mu} \leq 70\,\text{GeV}$. Signal yields are evaluated assuming $\mathcal{B}(h \to aa) = 10\%$ and $\mathcal{B}(aa \to \mu^+\mu^- b\bar{b}) = 1.7 \times 10^{-3}$, with the latter obtained in the context of type-3 2HDM+S with $\tan\beta = 2$.

	Z/γ^*+jets ($m_{\ell\ell} > 10\,\text{GeV}$)	$t\bar{t}\,(\ell\ell)$	Other
Backgrounds	210 ± 35	22 ± 1	3 ± 1
Total	235 ± 35		
Data	252		

	$m_a = 30\,\text{GeV}$	$m_a = 40\,\text{GeV}$	$m_a = 50\,\text{GeV}$	$m_a = 60\,\text{GeV}$
Signal	1.18	0.97	1.11	1.49

The signal yield is extracted using a fit to the reconstructed $m_{\mu\mu}$ distribution in data. The signal shape is modeled with a weighted sum of Voigt profile [82] and Crystal Ball [83] functions with a common mass parameter m_a,

$$S(m_{\mu\mu}|w,\sigma,\gamma,n,\sigma_{cb},\alpha,m_a) \equiv w\,V(m_{\mu\mu}|\sigma,\gamma,m_a) + (1-w)\,CB(m_{\mu\mu}|n,\sigma_{cb},\alpha,m_a). \quad (5)$$

The Voigt profile function, $V(m_{\mu\mu}|\sigma,\gamma,m_a)$, is a convolution of Lorentz and Gaussian profiles with γ and σ being the widths of the respective functions, both centered at m_a. The Crystal Ball function, $CB(m_{\mu\mu}|n,\sigma_{cb},\alpha,m_a)$, has a Gaussian core centered at m_a with a width of σ_{cb} together with a power-law low-end tail $A\,(B - (m_{\mu\mu} - m_a)/\sigma_{cb})^{-n}$ below a certain threshold α. The combination introduced in Eq. (5) is found to describe well the $m_{\mu\mu}$ distribution in the simulated signal samples.

The initial values for the signal model parameters are extracted from a simultaneous fit of the model to simulated signal samples with different pseudoscalar masses. All parameters in the signal model are found to be independent of m_a except σ and σ_{cb}, which show a linear dependence. The only floating parameter in these linear models are the slopes, s_σ and $s_{\sigma_{cb}}$ for σ and σ_{cb}, respectively. The signal model with the three free parameters, m_a, s_σ and $s_{\sigma_{cb}}$, is interpolated for mass hypotheses not covered by the simulated samples. The validity of the interpolation is checked within the $[25, 62.5]$ GeV range of the dimuon mass, and towards the boundaries.

The background is evaluated through a fit to the $m_{\mu\mu}$ distribution in data. The shape for the background is modeled with a set of analytical functions, using the discrete profiling method [9, 84, 85]. In this approach the choice of the functional form of the background shape is considered as a discrete nuisance parameter. This means that the likelihood function for the signal-plus-background fit has the form of

$$\mathcal{L}(\text{data}|\mu, \theta_\mu, b_\mu), \tag{6}$$

where μ is the measured quantity of signal, θ_μ are the corresponding nuisance parameters, and b_μ are the different background functions considered. Therefore, the uncertainty associated with the choice of the background model is treated in a similar way as other uncertainties associated with continuous nuisance parameters in the fit. The space of the background model contains multiple candidate models: different parametrizations of polynomials together with $1/P_n(x)$ functions where $P_n(x) \equiv x + \sum_{i=2}^{n} \alpha_i x^i$. The degree of polynomials in each category is determined through statistical tests to ensure the sufficiency of the number of parameters and to avoid overfitting the data [85]. Starting from the lowest degree for every candidate model, the necessity to increase the degree of the polynomial is examined. The model candidate with the higher degree is fit to data and a p-value is evaluated according to the number of degrees of freedom and the relative uncertainty of the parameters. Candidates with p-values below 5% are discarded.

The input background functions are used in the minimization of the negative logarithm of the likelihood with a penalty term added to account for the number of free parameters in the background model. The profile likelihood ratio for the penalized likelihood function can be written as

$$-2\ln\frac{\widetilde{\mathcal{L}}(\text{data}|\mu, \hat{\theta}_\mu, \hat{b}_\mu)}{\widetilde{\mathcal{L}}(\text{data}|\hat{\mu}, \hat{\theta}, \hat{b})}. \tag{7}$$

In this equation the numerator is the maximum penalized likelihood for a given μ, at the best-fit values of nuisance parameters, $\hat{\theta}_\mu$, and of the background function, $\hat{b}_\mu$. The denominator is the global maximum for $\widetilde{\mathcal{L}}$, achieved at $\mu = \hat{\mu}$, $\theta = \hat{\theta}$, and $b = \hat{b}$. A confidence interval on μ is obtained with the background function maximizing $\widetilde{\mathcal{L}}$ for any value of μ [84].

The analysis of data yields no significant excess of events over the SM background prediction. Figure 2 shows the $m_{\mu\mu}$ distribution in data together with the best fit output for a signal-plus-background model at $m_\mathrm{a} = 35\,\text{GeV}$. The relative difference between the expected limit of the best-fit background model and that of the unconditional fit is about 40%.

5 Search for $\mathrm{h} \to \mathrm{aa} \to 2\mu 2\tau$ decays

Five final states are studied in the $\mathrm{h} \to \mathrm{aa} \to 2\mu 2\tau$ channel, depending on whether the τ leptons decay to electrons (τ_e), to muons (τ_μ), or to hadrons (τ_h): $\mu^+\mu^-\tau_\mathrm{e}^+\tau_\mathrm{e}^-$, $\mu^+\mu^-\tau_\mathrm{e}^\pm\tau_\mu^\mp$, $\mu^+\mu^-\tau_\mathrm{e}^\pm\tau_\mathrm{h}^\mp$, $\mu^+\mu^-\tau_\mu^\pm\tau_\mathrm{h}^\mp$, or $\mu^+\mu^-\tau_\mathrm{h}^+\tau_\mathrm{h}^-$. The $\mu^+\mu^-\tau_\mu^+\tau_\mu^-$ final state is not considered due to the difficulty of correctly identifying the reconstructed muons as either direct pseudoscalar or τ decay products, which results in low sensitivity. Given the 2% dimuon mass resolution for the muons originating promptly from one of the a bosons arising from the h boson decay, an unbinned likelihood fit is performed to extract the results, using $m_{\mu\mu}$ as the observable. Pseudoscalar boson masses between 15 and 62.5 GeV are probed; the lower bound corresponds to the minimum mass that ensures a good signal efficiency with selection criteria that do not rely on boosted lepton pairs, and an expected background large enough to be modeled through techniques described below.

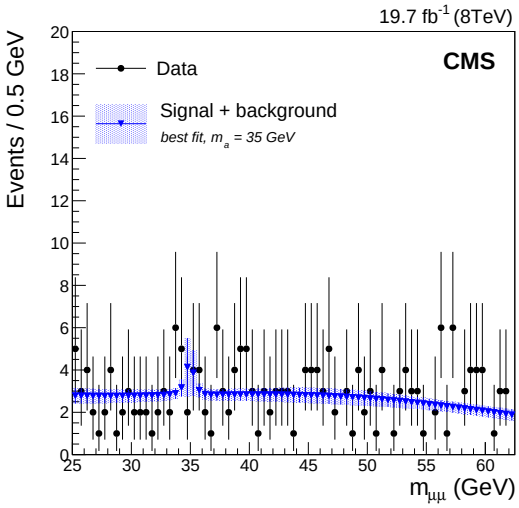

Figure 2: The best fit to the data for a signal-plus-background model with $m_a = 35\,\text{GeV}$, including profiling of the uncertainties, in the search for $h \to aa \to 2\mu 2b$ events.

5.1 Event selection

Events are selected using a double muon trigger relying on the presence of a muon with $p_T > 17$ GeV and another one with $p_T > 8$ GeV. For the offline selection, the leading muon p_T threshold is increased to 18 GeV, while the subleading muon p_T must exceed 9 GeV. To reconstruct the dimuon pair from the $a \to \mu^+\mu^-$ decay, two isolated muons of opposite charge, $p_T > 5\,\text{GeV}$, and $|\eta| < 2.4$ are selected. In the $\mu^+\mu^-\tau_e^+\tau_e^-$, $\mu^+\mu^-\tau_e^\pm\tau_h^\mp$ and $\mu^+\mu^-\tau_h^\pm\tau_h^\mp$ final states, where these are the only muons, their p_T thresholds are raised to 18 and 9 GeV to match the trigger requirements. If there are more than two muons in the final state, the highest-p_T muon is required to pass a p_T threshold of 18 GeV, and is considered as arising from the prompt decay of the light boson. It is then paired with the next highest-p_T muon of opposite charge. The other muons are considered to arise from leptonic decays of the τ lepton. The second highest-p_T muon is required to have p_T greater than 9 GeV. Muons are paired correctly in about 90% of the events for all masses. The $\tau\tau$ pair is reconstructed from a combination of oppositely charged identified and isolated muons, electrons, or τ_h, depending on the final state. The muons are selected with $p_T > 5\,\text{GeV}$ and $|\eta| < 2.4$, the electrons with $p_T > 7\,\text{GeV}$ and $|\eta| < 2.5$, and the τ_h candidates with $p_T > 15\,\text{GeV}$ and $|\eta| < 2.3$. The contribution from $h \to ZZ^* \to \mu^+\mu^-e^+e^-$ events is suppressed, in the $\mu^+\mu^-e^+e^-$ final state, by excluding events with visible invariant mass of the four leptons inside a 30 GeV-wide window around 125 GeV, the Higgs boson mass. The signal efficiency of this selection criterion is high since the four lepton invariant mass in $\mu^+\mu^-\tau_e^+\tau_e^-$ events is significantly reduced due to the presence of neutrinos in τ lepton decays.

The four objects are required to be separated from each other by at least $\Delta R = 0.4$. Events are discarded if they contain at least one jet that satisfies a b-tag requirement that allows $\mathcal{O}(0.1\%)$ of the light quark jets to survive, while the tag efficiency for genuine b jets is about 50%. This reduces the contribution from backgrounds with top quarks. To prevent a single event from contributing to different final states, events containing other identified and isolated electrons or muons in addition to the four selected objects are rejected; less than 1% of signal events are rejected because of this veto. Two selection criteria with a high signal efficiency are designed to reduce the contribution of the backgrounds to the signal region: the invariant mass of the $\mu\mu\tau\tau$ system is required to lie close to the Higgs boson mass ($|m_{\mu\mu\tau\tau} - 125\,\text{GeV}| < 25\,\text{GeV}$),

and the normalized difference between the masses of the di-τ and dimuon systems is required to be small ($|m_{\mu\mu} - m_{\tau\tau}|/m_{\mu\mu} < 0.8$). The $\tau\tau$ mass, $m_{\tau\tau}$, used to define both variables, is fully reconstructed with a maximum likelihood algorithm taking as input the four-momenta of the visible particles, as well as the $E_{\mathrm{T}}^{\mathrm{miss}}$ and its resolution [86]. This method gives a resolution of about 20% and 10%, for the $\tau\tau$ mass $m_{\tau\tau}$ and four-lepton mass $m_{\mu\mu\tau\tau}$, respectively. Finally, only events with a reconstructed dimuon mass between 14 and 66 GeV are considered in the study.

5.2 Signal and background estimation

Two types of backgrounds contribute to the signal region: irreducible ZZ production, and reducible processes with at least one jet being misidentified as one of the final-state leptons, mainly composed of Z+jets and WZ+jets events. The ZZ $\to 4\ell$ contribution, where ℓ denotes any charged lepton, is estimated from MC simulations, and the process is scaled to the NLO cross section [87]. The normalization and $m_{\mu\mu}$ distribution of the reducible processes are determined separately, using control samples in data. To estimate the normalization, the rates for jets to be misidentified as τ_{h}, electrons, or muons are measured in dedicated signal-free control regions, defined similarly to the signal region except that the τ candidates (electrons, muons, or τ_{h}) pass relaxed identification and isolation conditions and have SS charge. All misidentification rates are measured as a function of the p_{T} of the jet closest to the τ candidate, and are fitted using a decreasing exponential in addition to a constant term. Events with τ candidates passing the relaxed identification and isolation conditions, but not the signal region criteria, are scaled with weights that depend on the misidentification rates, to obtain an estimate of the yield of the reducible background in the signal region. The $m_{\mu\mu}$ distribution of reducible backgrounds is taken from a signal-free region in data, where both τ candidates have SS charge and pass relaxed identification and isolation criteria.

The dimuon mass distribution in signal events in final states with two muons is parameterized with a Voigt profile. In final states with three muons, the Gaussian component of the profile is found to be negligible, and the signal distributions are parameterized with Breit–Wigner profiles. A fit is performed for every final state and every generated a. To interpolate the signal distributions to any a boson in the studied mass range, the parameters of the fit functions are parameterized as a function of m_{a} by fitting with a third-degree polynomial the parameters of the Voigt or Breit–Wigner profiles obtained from the individual fits. A similar technique is used to interpolate the signal normalization to intermediate mass points; the parameterization leads to yield uncertainties for the signal between 5 and 8% depending on the final state. A closure test that consists of removing a signal sample corresponding to a given mass point from the parameterization of the Voigt and Lorentz fit parameters as a function of the mass, then comparing the parameterization interpolation to the direct fit to this sample, has demonstrated the validity of this technique. The ZZ irreducible background and reducible backgrounds are parameterized with Bernstein polynomials with five and three degrees of freedom respectively. The degrees of the polynomials are chosen to be the lowest that allow for a good agreement between the fit functions and the predicted backgrounds, according to f-tests. Uncertainties in the fit parameters of the Bernstein polynomials for reducible processes are taken into account in the statistical interpretation of results. They dominate over uncertainties associated with the choice of the fitting functions, which are neglected. Uncertainties in the ZZ background distribution are neglected given the low expected yield for this process relative to the reducible background contribution.

The parameterized dimuon mass distributions and the observed events after the complete selections are shown in Fig. 3 for the combination of the five final states. In this figure, the signal sample is normalized based on the Higgs boson cross section, σ_{h}, predicted in the SM. A

branching fraction of 10% is assumed for $h \to aa$. The a boson is assumed to decay only to leptons ($\mathcal{B}(a \to \tau^+\tau^-) + \mathcal{B}(a \to \mu^+\mu^-) + \mathcal{B}(a \to e^+e^-) = 1$), using Eq. (1). Combining all final states, 19 events are observed while 20.7 ± 2.2 are expected in the absence of signal. The expected signal yield, assuming the normalization described above, ranges from 3.1 to 8.2 events over the probed mass range, as detailed in Table 5.

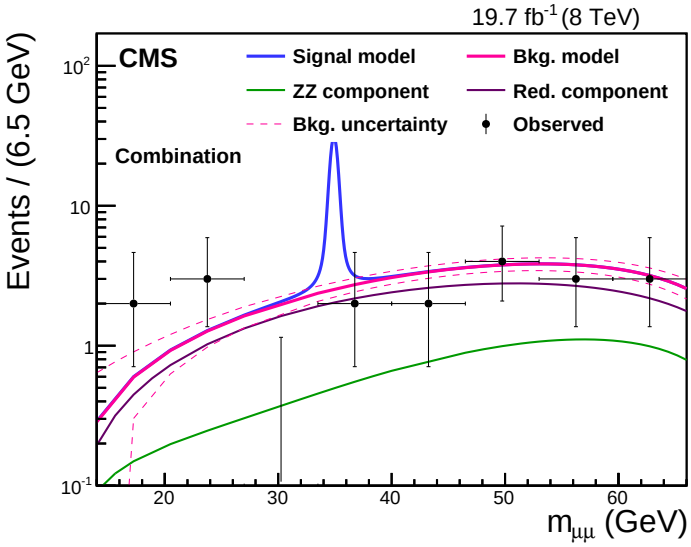

Figure 3: Background and signal ($m_a = 35\,\text{GeV}$) models, scaled to their expected yields, for the combination of all final states ($\mu^+\mu^-\tau_e^+\tau_e^-$, $\mu^+\mu^-\tau_e^\pm\tau_\mu^\mp$, $\mu^+\mu^-\tau_e^\pm\tau_h^\mp$, $\mu^+\mu^-\tau_\mu^\pm\tau_h^\mp$, and $\mu^+\mu^-\tau_h^+\tau_h^-$) in the search for $h \to aa \to 2\mu 2\tau$ decays. The two components of the background model, ZZ and reducible processes, are drawn. The signal sample is scaled with σ_h as predicted in the SM, assuming $\mathcal{B}(h \to aa) = 10\%$, and considering decays of the pseudoscalar a boson to leptons only ($\mathcal{B}(a \to \tau^+\tau^-) + \mathcal{B}(a \to \mu^+\mu^-) + \mathcal{B}(a \to e^+e^-) = 1$) using Eq. (1). The results are shown after a simultaneous maximum likelihood fit in all five channels that takes into account the systematic uncertainties described in Section 6.

6 Systematic uncertainties

The statistical interpretation of the analyses takes into account several sources of systematic uncertainties, included in the likelihood function as nuisance parameters following log-normal distributions in the case of yield uncertainties. Uncertainties related to the modeling of backgrounds estimated from data have already been discussed for the three independent analyses in Sections 3, 4, and 5, and will only be partially described here. Other systematic uncertainties are detailed in the following subsections, and summarized in Table 6.

6.1 Systematic uncertainties common to all analyses

Systematic uncertainties common to all analyses include the uncertainties in the trigger efficiency (between 0.2 and 4.2% depending on the analysis and on the process), the lepton identification and isolation efficiencies (6% for every τ_h [76], between 0.5 and 1.5% for muons, 2% for electrons), all evaluated with tag-and-probe methods [88] in Drell-Yan data and simulated samples. The uncertainties associated with the data-to-simulation correction factor for the b tagging efficiencies and misidentification rates are also propagated as systematic uncertain-

Table 5: Expected and observed yields in the search for h → aa → 2μ2τ decays. The signal samples are scaled with the production cross section for the SM h boson, assuming $\mathcal{B}(h \to aa) = 10\%$ and considering decays of the pseudoscalar a boson to leptons only. Background yields are obtained after a maximum likelihood fit to observed data, taking into account the systematic uncertainties detailed in Section 6.

	Signal		Backgrounds			Obs.
	$m_a = 20\,\text{GeV}$	$m_a = 60\,\text{GeV}$	ZZ	Reducible	Total	
$\mu^+\mu^-\tau_e^+\tau_e^-$	0.20±0.02	0.58±0.06	4.71±0.47	2.56±1.06	7.27±1.16	8
$\mu^+\mu^-\tau_e^\pm\tau_\mu^\mp$	0.58±0.08	1.42±0.16	0.10±0.01	1.68±0.70	1.78±0.70	2
$\mu^+\mu^-\tau_e^\pm\tau_h^\mp$	0.74±0.08	2.02±0.20	0.16±0.02	5.66±1.48	5.82±1.48	5
$\mu^+\mu^-\tau_\mu^\pm\tau_h^\mp$	0.96±0.10	2.30±0.22	0.13±0.02	0.91±0.28	1.14±0.29	1
$\mu^+\mu^-\tau_h^+\tau_h^-$	0.60±0.06	1.90±0.18	0.06±0.02	4.64±0.94	4.70±0.94	3
Combined	3.08±0.31	8.22±0.82	5.09±0.39	15.47±2.41	20.71±2.23	19

ties to the final results [75]. Uncertainties in the knowledge of the parton distribution functions [89, 90] are taken into account as yield uncertainties, and do not affect the shape of signal mass distributions. The uncertainty in the integrated luminosity amounts to 2.6%.

6.2 Systematic uncertainties for the h → aa → 4τ search

The leading systematic uncertainty in the h → aa → 4τ analysis comes from imperfect knowledge of the background composition in the signal region; it amounts to up to 90% of the background yield, as discussed in Section 3. Other sources of systematic uncertainty specific to this search affect the expected signal yield only. When added in quadrature to the background uncertainty, signal yield uncertainties account for at most 6 (10)% of the total uncertainty for $m_T \leq (>)\ 50\,\text{GeV}$. These minor uncertainties include an additional uncertainty of up to 10% related to the muon isolation if the trigger muon comes from a boosted $\tau_\mu\tau_X$ topology, as in the ggh, Zh, and VBF production modes, rather than an isolated W leptonic decay, as in the Wh mode. The signal yield is further affected by an asymmetric uncertainty in the τ charge misidentification probability of −1% and +2%. Up to 9.3% uncertainty in the signal yield is considered to account for uncertainties in the m_T computation because of uncertainties in the E_T^{miss} measurements. The b veto on the seed jet of the τ_X object introduces a maximum of 9.4% uncertainty in the signal yield. Finally, it should be noted that the full MC simulation and event reconstruction were only performed for the ggh and Wh samples with m_a = 5, 7, 9, 11, 13, and 15 GeV, and for the VBF and Zh samples with m_a = 9 GeV. The yields for the VBF (Zh) samples with m_a = 5, 7, 11, 13, and 15 GeV were extrapolated from the ggh(Wh) simulated samples at the corresponding pseudoscalar mass, which have similar final state kinematics. An uncertainty between 19% and 25%, depending on the production mode and m_T bin, is assigned to cover imperfect knowledge of the acceptance for the signals that were not simulated.

6.3 Systematic uncertainties for the h → aa → 2μ2b search

For the h → aa → 2μ2b analysis, the energy of jets is varied within a set of uncertainties depending on the jet p_T and η. This amounts to a 7% variation of the expected signal yield. The jet smearing corrections are altered within their uncertainties [74] to account for the uncertainty arising from the jet energy resolution, which has an effect on the process yield of about 1%. Furthermore, the uncertainty in the amount of pileup interactions per event is estimated by varying the total inelastic pp cross section [91] by ±5%. All sources of uncertainties including

Table 6: Sources of systematic uncertainties, and their effects on process yields, for the three different searches.

Source of uncertainty	Uncertainty in acceptance (%)		
	4τ	2μ2b	$2\mu2\tau$
Luminosity	2.6	2.6	2.6
Trigger efficiency	0.2-4.2	1.5	1
e identification	1	—	0-4
μ identification	0.5-1.5	3.5	2-3
+ for boosted $\tau_\mu\tau_X$ objects	10	—	—
τ_h identification	6	—	0-12
b tagging	0.2-9.4	0.1-4.5	1
Data-driven background estimation	59-84	discrete profiling	25-50 + shape unc.
Tau charge misidentification	2	—	—
$E_{\mathrm{T}}^{\mathrm{miss}}$ scale	1-9	—	—
VBF and Zh extrapolation	19-25	—	—
Jet energy scale	—	7	—
Jet energy resolution	—	0.10-0.15	—
Tau energy scale	—	—	0-10
Muon energy scale	—	3.5	Shape unc. only
ZZ simulation size	—	—	1-15
ZZ cross section	—	—	5+6

those associated with the muon energy scale and reconstruction and identification efficiencies are found to have a negligible effect on the signal modeling. The signal shape parameters are therefore left floating within their statistical uncertainties in the fit. The systematic uncertainty related to the discrete profiling method is small compared to the statistical uncertainty.

6.4 Systematic uncertainties for the $\mathrm{h} \to \mathrm{aa} \to 2\mu2\tau$ search

The effect of the τ_{h} energy scale in the $\mathrm{h} \to \mathrm{aa} \to 2\mu2\tau$ analysis is propagated to the mass distributions, and leads to uncertainties in the yields of the signal and of the irreducible background between 0 and 10%, depending on the final state. The muon energy scale uncertainty, amounting to 0.2%, is found to shift the mean of the signal distributions by up to 0.2%; this is taken into account as a parametric uncertainty in the mean of the signal distributions. Statistical uncertainties in the parameterization of the signal are accounted for through the uncertainties on the fit parameters describing the signal shape. The uncertainty in the normalization of the reducible background is obtained by varying the fit functions of the misidentification rates within their uncertainties. Uncertainties in background yields lie between 25 and 50%; uncertainties related to a given misidentification rate are correlated between corresponding final states. The number of events in the MC simulation of the ZZ background passing the full signal selection is small, and a statistical uncertainty ranging between 1 and 15% depending on the final state is considered to take this effect into account. This uncertainty is uncorrelated across all final states.

7 Results

7.1 Results of the search for $h \to aa \to 4\tau$ decays

The number of events observed in the signal window is compatible with the SM background prediction for the $h \to aa \to 4\tau$ analysis. Results are interpreted as upper limits on the production of $h \to aa$ relative to the SM Higgs boson production, scaled by $\mathcal{B}(h \to aa)\,\mathcal{B}^2(a \to \tau^+\tau^-) \equiv \mathcal{B}(h \to aa \to 4\tau)$. SM production cross sections are taken for ggh, Wh, Zh, and VBF processes [92]. Upper limits are calculated using the modified CL_s technique [93–96], in which the test statistic is a profile likelihood ratio. The asymptotic approximation is used to extract the results. In Figures 4, 5, and 6, the green (yellow) band labeled "$\pm 1(2)\sigma$ Expected" denotes the expected 68 (95)% C.L. band around the median upper limit if no data consistent with the signal expectation were to be observed.

The expected limits and the observed limit for the combination of the low- and high-m_T bin as a function of m_a are shown in Fig. 4. The sharp decrease in sensitivity between 5 and 7 GeV results from the 4 GeV $m_{\mu+X}$ signal requirement, which is less efficient for lower mass pseudoscalars.

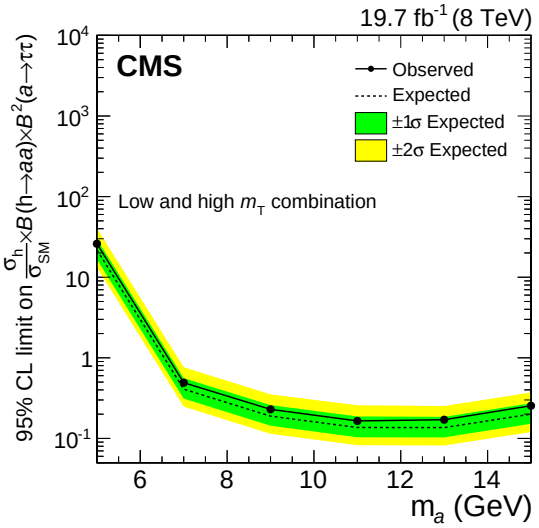

Figure 4: Observed 95% CL limits on the branching fraction $\mathcal{B}(h \to aa)\,\mathcal{B}^2(a \to \tau^+\tau^-)$ assuming SM h production rates, compared to expected limits for pseudoscalar mass points between 5 and 15 GeV.

7.2 Results of the search for $h \to aa \to 2\mu 2b$ decays

The analysis of the mass spectrum for the $h \to aa \to 2\mu 2b$ search does not show any significant excess of events over the SM background prediction either, as seen in Fig. 2. Upper limits on the production of $h \to aa$ relative to the SM Higgs boson ggh production mode, scaled by $\mathcal{B}(a \to b\bar{b})\,\mathcal{B}(a \to \mu^+\mu^-)$, are obtained at 95% CL with the asymptotic CL_s method. The observed and expected limits, together with the expected uncertainty bands, are illustrated in Fig. 5. The oscillations in the observed limit arise from the narrow dimuon mass resolution predicted for signal events.

7.3 Results of the search for $h \to aa \to 2\mu 2\tau$ decays

For the $h \to aa \to 2\mu 2\tau$ analysis, upper limits on the production of $h \to aa$ relative to the SM Higgs boson production (including ggh, VBF, Wh, Zh, and $t\bar{t}h$ production modes), scaled

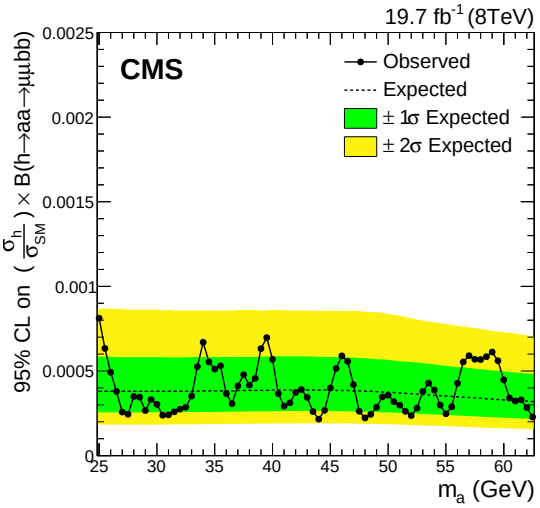

Figure 5: Observed and expected upper limits at 95% CL on the h boson production normalized to the SM prediction times $\mathcal{B}(\mathrm{h} \to \mathrm{aa} \to 2\mu 2\mathrm{b})$.

by $\mathcal{B}(\mathrm{a} \to \tau^+\tau^-)\,\mathcal{B}(\mathrm{a} \to \mu^+\mu^-)$, are set. An unbinned maximum likelihood fit to data is performed, and upper limits are set at 95% CL using the modified $\mathrm{CL_s}$ method, taking into account the different yield and shape systematic uncertainties described previously. The asymptotic approximation is not used in this case because of the low predicted background yields. The limits are shown in Fig. 6. Considering the large look-elsewhere effect [97] caused by the good dimuon mass resolution (about 2%), the wide mass range probed, and the number of studied final states, none of the observed events corresponds to an excess of more than two standard deviations in global significance. In particular, the deviation of the observed limit with respect to the expected limit in the $\mu^+\mu^-\tau_\mathrm{e}^\pm\tau_\mu^\mp$ final state comes from the presence of two observed events with a dimuon mass of 18.4 and 20.7 GeV, respectively, which lead to an excess of events with a maximum local significance of 3.5 standard deviations. Over the full mass range considered, the observed yield in this final state is compatible with the expected background yield of 1.80 ± 0.74 events. The uncertainty bands at low mass for most final states are narrow because of the low expected background yield.

7.4 Interpretation of $\mathrm{h} \to aa$ searches in 2HDM+S

Searches for non standard decays of the SM-like Higgs boson to a pair of light pseudoscalar bosons are interpreted in the context of 2HDM+S. In addition to the analyses presented in this paper, the results of two other searches are interpreted in this context: the $\mathrm{h} \to \mathrm{aa} \to 4\mu$ search covers pseudoscalar boson masses between 0.25 and 3.55 GeV [47], whereas another $\mathrm{h} \to \mathrm{aa} \to 4\tau$ search covers pseudoscalar masses between 4 and 8 GeV with different boosted τ lepton reconstruction techniques [48]. In 2HDM+S, the branching fractions of the light pseudoscalar a to SM particles depend on the model type and on $\tan\beta$. In type-1 2HDM+S, the fermionic couplings all have the same scaling with respect to the SM, whereas in type-2 2HDM+S (NMSSM-like), they are suppressed for down-type fermions for $\tan\beta < 1$ (and enhanced for $\tan\beta > 1$). In type-3 2HDM+S (lepton specific), the decays to leptons are enhanced with respect to the decays to quarks for $\tan\beta > 1$, and in type-4 2HDM+S (flipped), the decays to up-type quarks and leptons are enhanced for $\tan\beta < 1$.

Because $\mathcal{B}(\mathrm{a} \to \tau^+\tau^-)$ is directly proportional to $\mathcal{B}(\mathrm{a} \to \mu^+\mu^-)$ in any type of 2HDM+S as per Eq. (1), as is $\mathcal{B}(\mathrm{a} \to \mathrm{b\bar{b}})$ in type-1 and -2, the results of all analyses can be expressed as

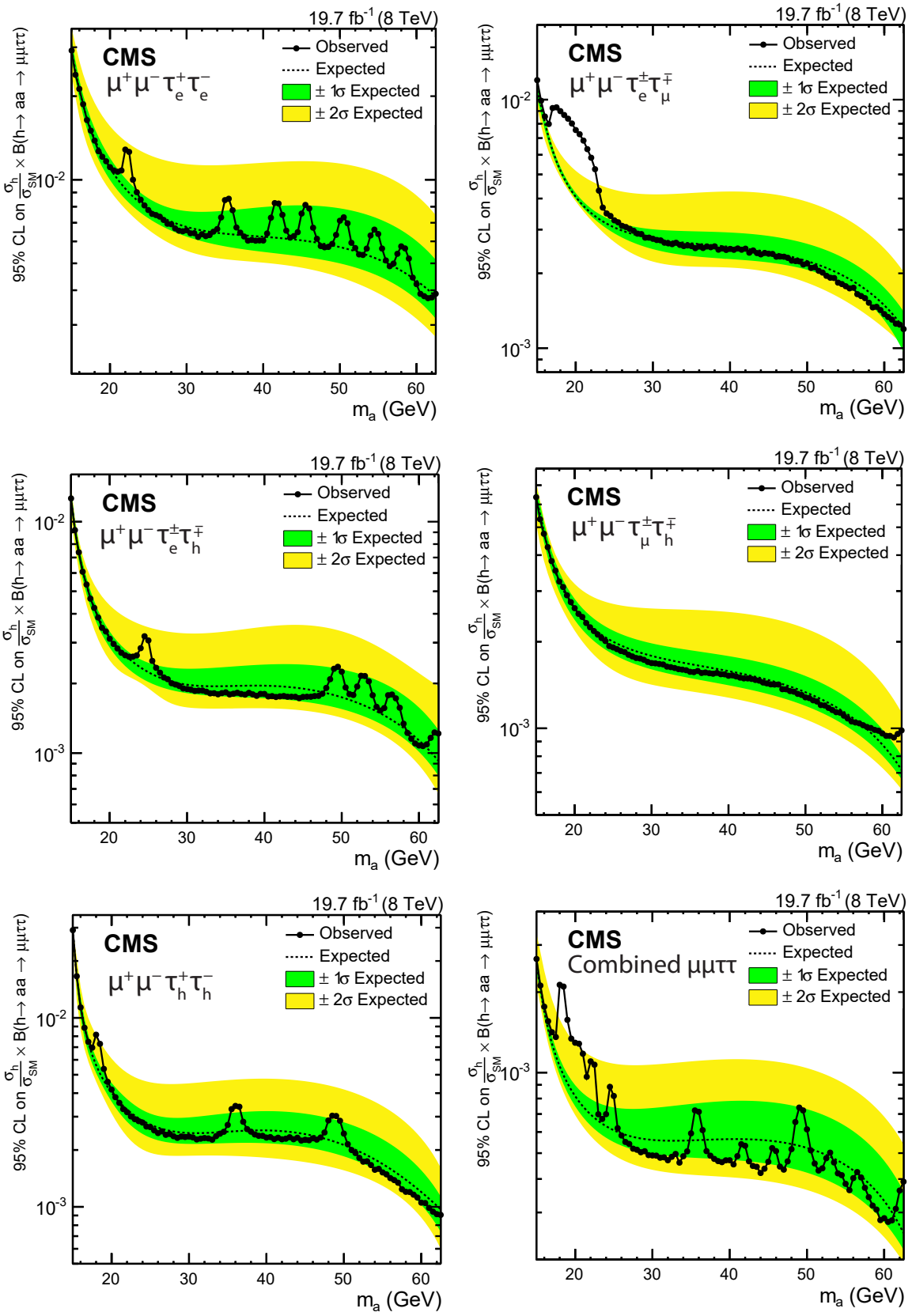

Figure 6: Expected and observed upper limits at 95% CL on the h boson production normalized to the SM prediction times $\mathcal{B}(\mathrm{h} \to \mathrm{aa} \to 2\mu 2\tau)$ in the $\mu^+\mu^-\tau_\mathrm{e}^+\tau_\mathrm{e}^-$ (upper left), $\mu^+\mu^-\tau_\mathrm{e}^\pm\tau_\mu^\mp$ (upper right), $\mu^+\mu^-\tau_\mathrm{e}^\pm\tau_\mathrm{h}^\mp$ (middle left), $\mu^+\mu^-\tau_\mu^\pm\tau_\mathrm{h}{}^\mp$ (middle right), and $\mu^+\mu^-\tau_\mathrm{h}{}^+\tau_\mathrm{h}{}^-$ (lower left) final states, and for the combination of these five final states (lower right). None of the event excesses exceed two standard deviations in global significance.

exclusion limits on $\frac{\sigma(h)}{\sigma_{SM}}\,\mathcal{B}(h \to aa)\,\mathcal{B}^2(a \to \mu^+\mu^-)$. This assumption is applied to obtain the results shown in Fig. 7. The exact value of $\mathcal{B}(a \to \mu^+\mu^-)$ depends on the type of 2HDM+S, on $\tan\beta$ and on the pseudoscalar boson mass. No significant excess of events is observed for any of the five analyses. Under type-1 and -2 2HDM+S hypothesis, the $h \to aa \to 2\mu 2b$ search is about one order of magnitude more sensitive than the $h \to aa \to 2\mu 2\tau$ search, but does not cover the pseudoscalar mass range between 15 and 25 GeV. Both $h \to aa \to 4\tau$ searches have a comparable sensitivity, in slightly different mass ranges.

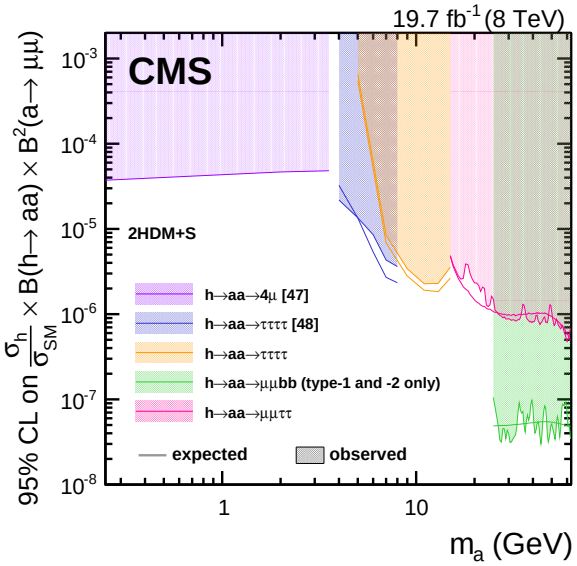

Figure 7: Expected and observed 95% CL exclusion limits on $(\sigma_h/\sigma_{SM})\,\mathcal{B}(h \to aa)\,\mathcal{B}^2(a \to \mu^+\mu^-)$ for various exotic h boson decay searches performed with data collected at 8 TeV with the CMS detector, assuming that the branching fractions of the pseudoscalar boson to muons, τ leptons and b quarks follow Eqs. (1)-(2). This assumption implies that the limit shown for $h \to aa \to 2\mu 2b$ is valid only in type-1 and -2 2HDM+S.

In 2HDM+S, the values of the branching fractions of the pseudoscalar boson to SM particles can be computed precisely, except for pseudoscalar boson masses between approximately 3 and 5 GeV and 9 and 11 GeV because of decays to quarkonia, and for pseudoscalar boson masses less than 1 GeV because of large QCD uncertainties in the hadronic final states [8]. We compute them following the prescriptions in Refs. [8, 46]. The branching fractions used to interpret the results in the four particular 2HDM+S scenarios described below are given in Table 7. Figure 8 (top left) shows the 95% CL in $(\sigma_h/\sigma_{SM})\,\mathcal{B}(h \to aa)$ in type-1 2HDM+S, for which there is no $\tan\beta$ dependence. Figure 8 (top right) shows corresponding limits in type-2 2HDM+S with $\tan\beta = 2$; the sensitivity of the $h \to aa \to 4\tau$ analyses is improved for $m_a < 2m_b$ because of the enhancement of the couplings to leptons. The $h \to aa \to 4\tau$ and $h \to aa \to 2\mu 2\tau$ analyses have low sensitivity in type-1 2HDM+S and type-2 2HDM+S with $\tan\beta = 2$ for $m_a > 2m_b$, because, in these scenarios, decays to b quarks dominate over decays to τ leptons and muons. The results in type-3 2HDM+S with $\tan\beta = 5$ are depicted in the bottom left part of Fig. 8; this scenario provides high sensitivity for the various analyses because of the enhancement of the couplings to leptons over those to quarks. Finally, the limits obtained in type-4 2HDM+S for $\tan\beta = 0.5$ are shown in the bottom right part of Fig. 8; the choice of $\tan\beta < 1$ ensures large couplings to leptons. Regions where the theoretical predictions for the branching fractions of the pseudoscalar boson to SM particles are not reliable are indicated with grey shaded areas

in the figure. To obtain the exclusion limit for $h \to aa \to 4\mu$ in these hypotheses, the model-independent limit shown in Fig. 7 is extrapolated from three mass points (0.25, 2.00, 3.55 GeV) to intermediate masses with a third degree polynomial, before being divided by the square of $\mathcal{B}(a \to \mu^+\mu^-)$. The variation of the limit around $m_a = 1.5$ GeV, visible in Fig. 8, is related to an increase of the pseudoscalar boson decay width to gluons because of the change in the number of active flavors in the QCD corrections and in the computation of the running of the strong coupling constant at a renormalization scale equal to m_a. The $b\bar{b}h$ production is neglected in this study. Its yield corresponds to less than 3% of the total production cross section for $\tan\beta < 5$, but could be larger for higher $\tan\beta$ values, or due to other new physics effects.

Table 7: Branching fractions of the pseudoscalar boson a to muons, τ leptons, and b quarks, in the four 2HDM+S scenarios considered in Fig. 8, as a function of the light boson mass. The branching fraction $\mathcal{B}(a \to b\bar{b})$ is not indicated in the mass range $m_a \in [5, 15]$ GeV because it is not used to interpret the results.

		$m_a \in [1, 3.5]$ GeV	$m_a \in [5, 15]$ GeV	$m_a \in [20, 62.5]$ GeV
Type-1	$\mathcal{B}(a \to \mu^+\mu^-)$	$4.6 \times 10^{-3} - 4.0 \times 10^{-2}$	$2.1 \times 10^{-4} - 1.8 \times 10^{-3}$	$2.0 \times 10^{-4} - 2.2 \times 10^{-4}$
	$\mathcal{B}(a \to \tau^+\tau^-)$	0	$5.7 \times 10^{-2} - 3.6 \times 10^{-1}$	$5.5 \times 10^{-2} - 6.3 \times 10^{-2}$
	$\mathcal{B}(a \to b\bar{b})$	0	—	$8.3 \times 10^{-1} - 8.8 \times 10^{-1}$
Type-2 $\tan\beta = 2$	$\mathcal{B}(a \to \mu^+\mu^-)$	$2.5 \times 10^{-2} - 3.8 \times 10^{-2}$	$2.2 \times 10^{-4} - 4.0 \times 10^{-3}$	$2.1 \times 10^{-4} - 2.5 \times 10^{-4}$
	$\mathcal{B}(a \to \tau^+\tau^-)$	0	$6.0 \times 10^{-2} - 7.9 \times 10^{-1}$	$5.8 \times 10^{-2} - 7.0 \times 10^{-2}$
	$\mathcal{B}(a \to b\bar{b})$	0	—	$9.2 \times 10^{-1} - 9.3 \times 10^{-1}$
Type-3 $\tan\beta = 5$	$\mathcal{B}(a \to \mu^+\mu^-)$	$7.4 \times 10^{-1} - 9.6 \times 10^{-1}$	$3.5 \times 10^{-3} - 5.0 \times 10^{-3}$	$3.4 \times 10^{-3} - 3.5 \times 10^{-3}$
	$\mathcal{B}(a \to \tau^+\tau^-)$	0	$9.1 \times 10^{-1} - 9.9 \times 10^{-1}$	9.7×10^{-1}
	$\mathcal{B}(a \to b\bar{b})$	0	—	$2.0 \times 10^{-2} - 2.5 \times 10^{-2}$
Type-4 $\tan\beta = 0.5$	$\mathcal{B}(a \to \mu^+\mu^-)$	$4.5 \times 10^{-3} - 1.4 \times 10^{-1}$	$1.2 \times 10^{-3} - 1.8 \times 10^{-3}$	$1.1 \times 10^{-3} - 1.2 \times 10^{-3}$
	$\mathcal{B}(a \to \tau^+\tau^-)$	0	$3.2 \times 10^{-1} - 3.5 \times 10^{-1}$	$3.0 \times 10^{-1} - 3.3 \times 10^{-1}$
	$\mathcal{B}(a \to b\bar{b})$	0	—	$2.5 \times 10^{-1} - 3.2 \times 10^{-1}$

The $h \to aa \to 2\mu 2b$ and $h \to aa \to 2\mu 2\tau$ analyses are complementary over the $\tan\beta$ spectrum in type-3 and -4 2HDM+S, where the ratio of the branching fractions of the pseudoscalar boson to τ leptons and b quarks depends on $\tan\beta$. The former search is more sensitive in type-3 2HDM+S for $\tan\beta \lesssim 2.2$ and in type-4 2HDM+S for $\tan\beta \gtrsim 0.8$, as shown in Fig. 9.

The best limits on $\frac{\sigma_h}{\sigma_{SM}}\mathcal{B}(h \to aa)$ are obtained in type-3 2HDM+S with large $\tan\beta$ values for the $h \to aa \to 4\tau$ and $h \to aa \to 2\mu 2\tau$ analyses. As shown in Fig. 8 (bottom left), upper limits at 95% CL as low as 17% for the $h \to aa \to 4\tau$ analysis and 4% for the $h \to aa \to 2\mu 2\tau$ analysis can be set for $\tan\beta = 5$. Similarly low limits are achieved at higher $\tan\beta$. The best limit for the $h \to aa \to 2\mu 2b$ analysis is 16%, and is obtained in type-3 2HDM+S too, but with $\tan\beta = 2$ as shown in Fig. 9 (left).

8 Summary

Searches for the decay of the SM-like Higgs boson to pairs of light scalar particles have been performed using 19.7 fb^{-1} of pp collisions at a center-of-mass energy of 8 TeV, collected by the CMS experiment at the LHC, in final states with τ leptons, muons, or b quark jets. Such signatures are motivated in light of the non-negligible branching fraction provided in recent experimental constraints for non-SM h decays. The data were found to be compatible with SM predictions. Whereas indirect measurements from the combination of data collected by the

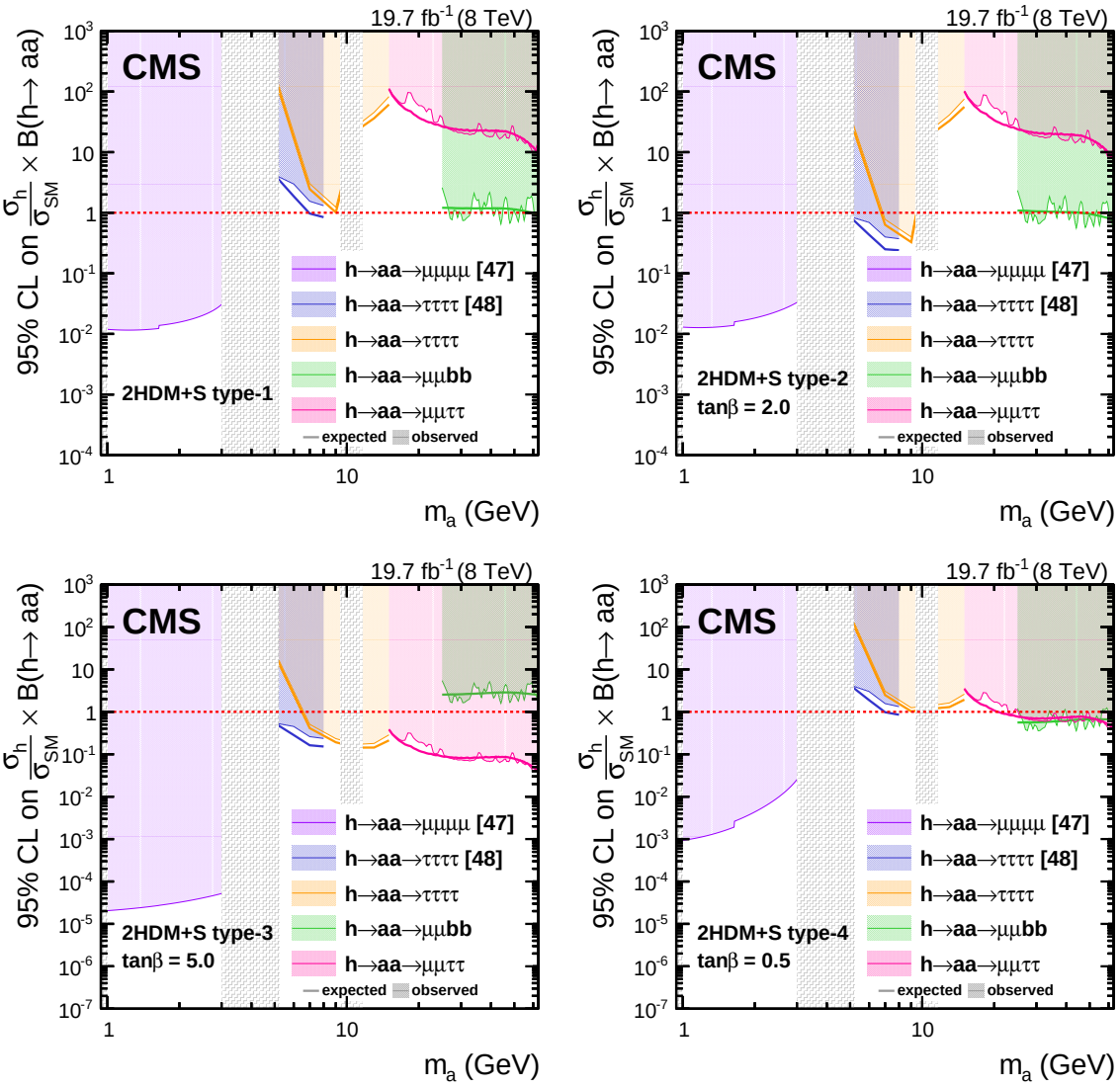

Figure 8: Expected and observed 95% CL limits on $(\sigma_{\mathrm{h}}/\sigma_{\mathrm{SM}})\,\mathcal{B}(\mathrm{h} \to \mathrm{aa})$ in 2HDM+S type-1 (top left), type-2 with $\tan\beta = 2$ (top right), type-3 with $\tan\beta = 5$ (bottom left), and type-4 with $\tan\beta = 0.5$ (bottom right). Limits are shown as a function of the mass of the light boson, m_{a}. The branching fractions of the pseudoscalar boson to SM particles are computed following a model described in Ref. [8]. Grey shaded regions correspond to regions where theoretical predictions for the branching fractions of the pseudoscalar boson to SM particles are not reliable.

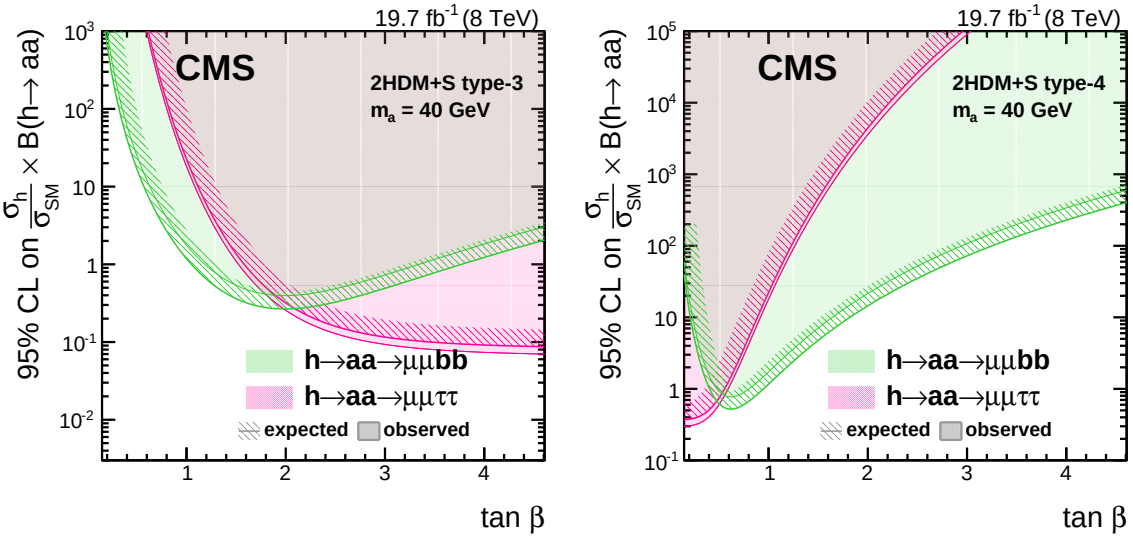

Figure 9: The 95% CL limit on $(\sigma_{\mathrm{h}}/\sigma_{\mathrm{SM}})\,\mathcal{B}(\mathrm{h}\to\mathrm{aa})$ in 2HDM+S type-3 (left) and type-4 (right) for different $\tan\beta$ values, for the $\mathrm{h}\to\mathrm{aa}\to 2\mu 2\tau$ and $\mathrm{h}\to\mathrm{aa}\to 2\mu 2\mathrm{b}$ analyses at $m_{\mathrm{a}} = 40\,\mathrm{GeV}$. The branching fractions of the pseudoscalar boson to SM particles are computed following the prescriptions in Ref. [8].

ATLAS and CMS collaborations at the LHC at 8 TeV center-of-mass energy set an upper limit of 34% on branching fraction of the Higgs boson to BSM, direct limits provide complementarity and improve the sensitivity to the 2HDM+S models for particular scenarios and pseudoscalar masses. Upper limits at 95% CL on $(\sigma_{\mathrm{h}}/\sigma_{\mathrm{SM}})\,\mathcal{B}(\mathrm{h}\to\mathrm{aa})$, assuming SM production of the 125 GeV Higgs boson, are as low as 17, 16, and 4%, and have been determined for the $\mathrm{h}\to\mathrm{aa}\to 4\tau$, $\mathrm{h}\to\mathrm{aa}\to 2\mu 2\mathrm{b}$, and $\mathrm{h}\to\mathrm{aa}\to 2\mu 2\tau$ analyses, respectively.

Acknowledgments

We congratulate our colleagues in the CERN accelerator departments for the excellent performance of the LHC and thank the technical and administrative staffs at CERN and at other CMS institutes for their contributions to the success of the CMS effort. In addition, we gratefully acknowledge the computing centers and personnel of the Worldwide LHC Computing Grid for delivering so effectively the computing infrastructure essential to our analyses. Finally, we acknowledge the enduring support for the construction and operation of the LHC and the CMS detector provided by the following funding agencies: the Austrian Federal Ministry of Science, Research and Economy and the Austrian Science Fund; the Belgian Fonds de la Recherche Scientifique, and Fonds voor Wetenschappelijk Onderzoek; the Brazilian Funding Agencies (CNPq, CAPES, FAPERJ, and FAPESP); the Bulgarian Ministry of Education and Science; CERN; the Chinese Academy of Sciences, Ministry of Science and Technology, and National Natural Science Foundation of China; the Colombian Funding Agency (COLCIENCIAS); the Croatian Ministry of Science, Education and Sport, and the Croatian Science Foundation; the Research Promotion Foundation, Cyprus; the Secretariat for Higher Education, Science, Technology and Innovation, Ecuador; the Ministry of Education and Research, Estonian Research Council via IUT23-4 and IUT23-6 and European Regional Development Fund, Estonia; the Academy of Finland, Finnish Ministry of Education and Culture, and Helsinki Institute of Physics; the Institut National de Physique Nucléaire et de Physique des Particules / CNRS, and Commissariat à l'Énergie Atomique et aux Énergies Alternatives / CEA, France; the Bundes-

ministerium für Bildung und Forschung, Deutsche Forschungsgemeinschaft, and Helmholtz-Gemeinschaft Deutscher Forschungszentren, Germany; the General Secretariat for Research and Technology, Greece; the National Scientific Research Foundation, and National Innovation Office, Hungary; the Department of Atomic Energy and the Department of Science and Technology, India; the Institute for Studies in Theoretical Physics and Mathematics, Iran; the Science Foundation, Ireland; the Istituto Nazionale di Fisica Nucleare, Italy; the Ministry of Science, ICT and Future Planning, and National Research Foundation (NRF), Republic of Korea; the Lithuanian Academy of Sciences; the Ministry of Education, and University of Malaya (Malaysia); the Mexican Funding Agencies (BUAP, CINVESTAV, CONACYT, LNS, SEP, and UASLP-FAI); the Ministry of Business, Innovation and Employment, New Zealand; the Pakistan Atomic Energy Commission; the Ministry of Science and Higher Education and the National Science Centre, Poland; the Fundação para a Ciência e a Tecnologia, Portugal; JINR, Dubna; the Ministry of Education and Science of the Russian Federation, the Federal Agency of Atomic Energy of the Russian Federation, Russian Academy of Sciences, the Russian Foundation for Basic Research and the Russian Competitiveness Program of NRNU MEPhI (M.H.U.); the Ministry of Education, Science and Technological Development of Serbia; the Secretaría de Estado de Investigación, Desarrollo e Innovación and Programa Consolider-Ingenio 2010, Spain; the Swiss Funding Agencies (ETH Board, ETH Zurich, PSI, SNF, UniZH, Canton Zurich, and SER); the Ministry of Science and Technology, Taipei; the Thailand Center of Excellence in Physics, the Institute for the Promotion of Teaching Science and Technology of Thailand, Special Task Force for Activating Research and the National Science and Technology Development Agency of Thailand; the Scientific and Technical Research Council of Turkey, and Turkish Atomic Energy Authority; the National Academy of Sciences of Ukraine, and State Fund for Fundamental Researches, Ukraine; the Science and Technology Facilities Council, UK; the US Department of Energy, and the US National Science Foundation.

Individuals have received support from the Marie-Curie program and the European Research Council and EPLANET (European Union); the Leventis Foundation; the A. P. Sloan Foundation; the Alexander von Humboldt Foundation; the Belgian Federal Science Policy Office; the Fonds pour la Formation à la Recherche dans l'Industrie et dans l'Agriculture (FRIA-Belgium); the Agentschap voor Innovatie door Wetenschap en Technologie (IWT-Belgium); the Ministry of Education, Youth and Sports (MEYS) of the Czech Republic; the Council of Science and Industrial Research, India; the HOMING PLUS program of the Foundation for Polish Science, cofinanced from European Union, Regional Development Fund, the Mobility Plus program of the Ministry of Science and Higher Education, the National Science Center (Poland), contracts Harmonia 2014/14/M/ST2/00428, Opus 2014/13/B/ST2/02543, 2014/15/B/ST2/03998, and 2015/19/B/ST2/02861, Sonata-bis 2012/07/E/ST2/01406; the Thalis and Aristeia programs cofinanced by EU-ESF and the Greek NSRF; the National Priorities Research Program by Qatar National Research Fund; the Programa Clarín-COFUND del Principado de Asturias; the Rachadapisek Sompot Fund for Postdoctoral Fellowship, Chulalongkorn University and the Chulalongkorn Academic into Its 2nd Century Project Advancement Project (Thailand); and the Welch Foundation, contract C-1845.

References

[1] ATLAS Collaboration, "Observation of a new particle in the search for the Standard Model Higgs boson with the ATLAS detector at the LHC", *Phys. Lett. B* **716** (2012) 1, doi:10.1016/j.physletb.2012.08.020, arXiv:1207.7214.

[2] CMS Collaboration, "Observation of a new boson at a mass of 125 GeV with the CMS experiment at the LHC", *Phys. Lett. B* **716** (2012) 30, doi:10.1016/j.physletb.2012.08.021, arXiv:1207.7235.

[3] CMS Collaboration, "Observation of a new boson with mass near 125 GeV in pp collisions at $\sqrt{s} = 7$ and 8 TeV", *JHEP* **06** (2013) 081, doi:10.1007/JHEP06(2013)081, arXiv:1303.4571.

[4] ATLAS and CMS Collaborations, "Measurements of the Higgs boson production and decay rates and constraints on its couplings from a combined ATLAS and CMS analysis of the LHC pp collision data at $\sqrt{s} = 7$ and 8 TeV", *JHEP* **08** (2016) 45, doi:10.1007/JHEP08(2016)045, arXiv:1606.02266.

[5] CMS Collaboration, "Precise determination of the mass of the Higgs boson and tests of compatibility of its couplings with the standard model predictions using proton collisions at 7 and 8 TeV", *Eur. Phys. J. C* **75** (2015) 212, doi:10.1140/epjc/s10052-015-3351-7, arXiv:1412.8662.

[6] ATLAS Collaboration, "Measurements of the Higgs boson production and decay rates and coupling strengths using pp collision data at $\sqrt{s} = 7$ and 8 TeV in the ATLAS experiment", *Eur. Phys. J. C* **76** (2016) 6, doi:10.1140/epjc/s10052-015-3769-y, arXiv:1507.04548.

[7] ATLAS Collaboration, "Constraints on new phenomena via Higgs boson couplings and invisible decays with the ATLAS detector", *JHEP* **11** (2015) 206, doi:10.1007/JHEP11(2015)206, arXiv:1509.00672.

[8] D. Curtin et al., "Exotic decays of the 125 GeV Higgs boson", *Phys. Rev. D* **90** (2014) 075004, doi:10.1103/PhysRevD.90.075004, arXiv:1312.4992.

[9] ATLAS and CMS Collaborations, "Combined measurement of the Higgs boson mass in pp collisions at $\sqrt{s} = 7$ and 8 TeV with the ATLAS and CMS experiments", *Phys. Rev. Lett.* **114** (2015) 191803, doi:10.1103/PhysRevLett.114.191803, arXiv:1503.07589.

[10] M. E. Peskin, "Comparison of LHC and ILC capabilities for Higgs boson coupling measurements", (2012). arXiv:1207.2516.

[11] CMS Collaboration, "Projected performance of an upgraded CMS detector at the LHC and HL-LHC: contribution to the Snowmass process", (2013). arXiv:1307.7135.

[12] ATLAS Collaboration, "Physics at a high-luminosity LHC with ATLAS", (2013). arXiv:1307.7292.

[13] R. Dermisek and J. F. Gunion, "Escaping the large fine tuning and little hierarchy problems in the next to minimal supersymmetric model and $h \to aa$ decays", *Phys. Rev. Lett.* **95** (2005) 041801, doi:10.1103/PhysRevLett.95.041801, arXiv:hep-ph/0502105.

[14] R. Dermisek and J. F. Gunion, "The NMSSM close to the R-symmetry limit and naturalness in $h \to aa$ decays for $m_a < 2m_b$", *Phys. Rev. D* **75** (2007) 075019, doi:10.1103/PhysRevD.75.075019, arXiv:hep-ph/0611142.

[15] S. Chang, R. Dermisek, J. F. Gunion, and N. Weiner, "Nonstandard Higgs boson decays", *Ann. Rev. Nucl. Part. Sci.* **58** (2008) 75, doi:10.1146/annurev.nucl.58.110707.171200, arXiv:0801.4554.

[16] C. Englert, T. Plehn, D. Zerwas, and P. M. Zerwas, "Exploring the Higgs portal", *Phys. Lett. B* **703** (2011) 298, doi:10.1016/j.physletb.2011.08.002, arXiv:1106.3097.

[17] T. D. Lee, "A theory of spontaneous T violation", *Phys. Rev. D* **8** (1973) 1226, doi:10.1103/PhysRevD.8.1226.

[18] N. G. Deshpande and E. Ma, "Pattern of symmetry breaking with two higgs doublets", *Phys. Rev. D* **18** (1978) 2574, doi:10.1103/PhysRevD.18.2574.

[19] N. G. Deshpande and E. Ma, "The fermion mass scale and possible effects of higgs bosons on experimental observables", *Nucl. Phys. B* **161** (1979) 493, doi:10.1016/0550-3213(79)90225-6.

[20] J. F. Gunion, H. E. Haber, G. L. Kane, and S. Dawson, "The Higgs hunter's guide", volume 80 of *Frontiers in Physics*. Perseus Books, 2000.

[21] G. C. Branco et al., "Theory and phenomenology of two-Higgs-doublet models", *Phys. Rep.* **516** (2012) 1, doi:10.1016/j.physrep.2012.02.002, arXiv:1106.0034.

[22] P. Fayet, "Supergauge invariant extension of the Higgs mechanism and a model for the electron and its neutrino", *Nucl. Phys. B* **90** (1975) 104, doi:10.1016/0550-3213(75)90636-7.

[23] P. Fayet, "Spontaneously broken supersymmetric theories of weak, electromagnetic and strong interactions", *Phys. Lett. B* **69** (1977) 489, doi:10.1016/0370-2693(77)90852-8.

[24] J. E. Kim and H. P. Nilles, "The μ-problem and the strong CP-problem", *Phys. Lett. B* **138** (1984) 150, doi:10.1016/0370-2693(84)91890-2.

[25] U. Ellwanger, C. Hugonie, and A. M. Teixeira, "The next-to-minimal supersymmetric standard model", *Phys. Rep.* **496** (2010) 1, doi:10.1016/j.physrep.2010.07.001, arXiv:0910.1785.

[26] J. Bernon, J. F. Gunion, Y. Jiang, and S. Kraml, "Light Higgs bosons in two-Higgs-doublet models", *Phys. Rev. D* **91** (2015) 075019, doi:10.1103/PhysRevD.91.075019, arXiv:1412.3385.

[27] R. D. Peccei and H. R. Quinn, "CP conservation in the presence of instantons", *Phys. Rev. Lett.* **38** (1977) 1440, doi:10.1103/PhysRevLett.38.1440.

[28] R. D. Peccei and H. R. Quinn, "Constraints imposed by CP conservation in the presence of instantons", *Phys. Rev. D* **16** (1977) 1791, doi:10.1103/PhysRevD.16.1791.

[29] P. Fayet, "Supersymmetry and weak, electromagnetic and strong interactions", *Phys. Lett. B* **64** (1976) 159, doi:10.1016/0370-2693(76)90319-1.

[30] S. Heinemeyer, O. Stal, and G. Weiglein, "Interpreting the LHC Higgs search results in the MSSM", *Phys. Lett. B* **710** (2012) 201, doi:10.1016/j.physletb.2012.02.084, arXiv:1112.3026.

[31] A. Celis, V. Ilisie, and A. Pich, "LHC constraints on two-Higgs doublet models", *JHEP* **07** (2013) 053, doi:10.1007/JHEP07(2013)053, arXiv:1302.4022.

[32] B. Grinstein and P. Uttayarat, "Carving out parameter space in type-II two Higgs doublets model", *JHEP* **06** (2013) 094, doi:10.1007/JHEP06(2013)094, arXiv:1304.0028.

[33] B. Coleppa, F. Kling, and S. Su, "Constraining type-II 2HDM in light of LHC Higgs searches", *JHEP* **01** (2014) 161, doi:10.1007/JHEP01(2014)161, arXiv:1305.0002.

[34] C.-Y. Chen, S. Dawson, and M. Sher, "Heavy Higgs searches and constraints on two Higgs doublet models", *Phys. Rev. D* **88** (2013) 015018, doi:10.1103/PhysRevD.88.015018, arXiv:1305.1624.

[35] N. Craig, J. Galloway, and S. Thomas, "Searching for signs of the second Higgs doublet", (2013). arXiv:1305.2424.

[36] L. Wang and X.-F. Han, "Status of the aligned two-Higgs-doublet model confronted with the Higgs data", *JHEP* **04** (2014) 128, doi:10.1007/JHEP04(2014)128, arXiv:1312.4759.

[37] J. Baglio, O. Eberhardt, U. Nierste, and M. Wiebusch, "Benchmarks for Higgs pair production and heavy Higgs searches in the two-Higgs-doublet model of type II", *Phys. Rev. D* **90** (2014) 015008, doi:10.1103/PhysRevD.90.015008, arXiv:1403.1264.

[38] B. Dumont, J. F. Gunion, Y. Jiang, and S. Kraml, "Constraints on and future prospects for two-Higgs-doublet models in light of the LHC Higgs signal", *Phys. Rev. D* **90** (2015) 035021, doi:10.1103/PhysRevD.90.035021, arXiv:1405.3584.

[39] S. F. King, M. Muehlleitner, R. Nevzorov, and K. Walz, "Natural NMSSM Higgs bosons", *Nucl. Phys. B* **870** (2013) 323, doi:10.1016/j.nuclphysb.2013.01.020, arXiv:1211.5074.

[40] J. Cao et al., "A light Higgs scalar in the NMSSM confronted with the latest LHC Higgs data", *JHEP* **11** (2013) 018, doi:10.1007/JHEP11(2013)018, arXiv:1309.4939.

[41] N. D. Christensen, T. Han, Z. Liu, and S. Su, "Low-mass Higgs bosons in the NMSSM and their LHC implications", *JHEP* **08** (2013) 019, doi:10.1007/JHEP08(2013)019, arXiv:1303.2113.

[42] D. G. Cerdeno, P. Ghosh, and C. B. Park, "Probing the two light Higgs scenario in the NMSSM with a low-mass pseudoscalar", *JHEP* **06** (2013) 031, doi:10.1007/JHEP06(2013)031, arXiv:1301.1325.

[43] G. Chalons and F. Domingo, "Analysis of the Higgs potentials for two doublets and a singlet", *Phys. Rev. D* **86** (2012) 115024, doi:10.1103/PhysRevD.86.115024, arXiv:1209.6235.

[44] A. Ahriche, A. Arhrib, and S. Nasri, "Higgs phenomenology in the two-singlet model", *JHEP* **02** (2014) 042, doi:10.1007/JHEP02(2014)042, arXiv:1309.5615.

[45] J. Bernon et al., "Scrutinizing the alignment limit in two-Higgs-doublet models: $m_{\mathrm{h}} = 125\,\mathrm{GeV}$", *Phys. Rev. D* **92** (2015) 075004, doi:10.1103/PhysRevD.92.075004, arXiv:1507.00933.

[46] A. Djouadi, "The anatomy of electro-weak symmetry breaking. I: the Higgs boson in the standard model", *Phys. Rep.* **457** (2008) 1, doi:10.1016/j.physrep.2007.10.004, arXiv:hep-ph/0503172.

[47] CMS Collaboration, "A search for pair production of new light bosons decaying into muons", *Phys. Lett. B* **752** (2016) 146, doi:10.1016/j.physletb.2015.10.067, arXiv:1506.00424.

[48] CMS Collaboration, "Search for a very light NMSSM Higgs boson produced in decays of the 125 GeV scalar boson and decaying into tau leptons in pp collisions at $\sqrt{s} = 8\,\mathrm{TeV}$", *JHEP* **01** (2016) 079, doi:10.1007/JHEP01(2016)079, arXiv:1510.06534.

[49] D0 Collaboration, "Search for NMSSM Higgs bosons in the $h \to aa \to \mu\mu\mu\mu, \mu\mu\tau\tau$ channels using $p\bar{p}$ collisions at $\sqrt{s} = 1.96\,\mathrm{TeV}$", *Phys. Rev. Lett.* **103** (2009) 061801, doi:10.1103/PhysRevLett.103.061801, arXiv:0905.3381.

[50] ATLAS Collaboration, "Search for Higgs bosons decaying to aa in the $\mu\mu\tau\tau$ final state in pp collisions at $\sqrt{s} = 8\,\mathrm{TeV}$ with the ATLAS experiment", *Phys. Rev. D* **92** (2015) 052002, doi:10.1103/PhysRevD.92.052002, arXiv:1505.01609.

[51] CMS Collaboration, "Search for a light pseudoscalar Higgs boson in the dimuon decay channel in pp collisions at $\sqrt{s} = 7\,\mathrm{TeV}$", *Phys. Rev. Lett.* **109** (2012) 121801, doi:10.1103/PhysRevLett.109.121801, arXiv:1206.6326.

[52] CMS Collaboration, "Search for a low-mass pseudoscalar Higgs boson produced in association with a $\mathrm{b\bar{b}}$ pair in pp collisions at $\sqrt{s} = 8\,\mathrm{TeV}$", *Phys. Lett. B* **758** (2016) 296, doi:10.1016/j.physletb.2016.05.003, arXiv:1511.03610.

[53] CMS Collaboration, "The CMS experiment at the CERN LHC", *JINST* **3** (2008) S08004, doi:10.1088/1748-0221/3/08/S08004.

[54] J. Alwall et al., "MadGraph 5: going beyond", *JHEP* **06** (2011) 128, doi:10.1007/JHEP06(2011)128, arXiv:1106.0522.

[55] T. Sjöstrand, S. Mrenna, and P. Z. Skands, "PYTHIA 6.4 physics and manual", *JHEP* **05** (2006) 026, doi:10.1088/1126-6708/2006/05/026, arXiv:hep-ph/0603175.

[56] Z. Wąs, "TAUOLA the library for τ lepton decay, and KKMC/KORALB/KORALZ/... status report", *Nucl. Phys. Proc. Suppl.* **98** (2001) 96, doi:10.1016/S0920-5632(01)01200-2, arXiv:hep-ph/0011305.

[57] S. Alioli, P. Nason, C. Oleari, and E. Re, "NLO single-top production matched with shower in POWHEG: s- and t-channel contributions", *JHEP* **09** (2009) 111, doi:10.1088/1126-6708/2009/09/111, arXiv:0907.4076. [Erratum: doi:10.1007/JHEP02(2010)011].

[58] S. Alioli, P. Nason, C. Oleari, and E. Re, "A general framework for implementing NLO calculations in shower Monte Carlo programs: the POWHEG BOX", *JHEP* **06** (2010) 043, doi:10.1007/JHEP06(2010)043, arXiv:1002.2581.

[59] E. Re, "Single-top Wt-channel production matched with parton showers using the POWHEG method", *Eur. Phys. J. C* **71** (2011) 1547, doi:10.1140/epjc/s10052-011-1547-z, arXiv:1009.2450.

[60] S. Frixione, P. Nason, and C. Oleari, "Matching NLO QCD computations with parton shower simulations: the POWHEG method", *JHEP* **11** (2007) 070, doi:10.1088/1126-6708/2007/11/070, arXiv:0709.2092.

[61] J. Pumplin et al., "New generation of parton distributions with uncertainties from global QCD analysis", *JHEP* **07** (2002) 012, doi:10.1088/1126-6708/2002/07/012, arXiv:hep-ph/0201195.

[62] GEANT4 Collaboration, "GEANT4—a simulation toolkit", *Nucl. Instrum. Meth. A* **506** (2003) 250, doi:10.1016/S0168-9002(03)01368-8.

[63] GEANT4 Collaboration, "Geant4 developments and applications", *IEEE Trans. Nucl. Sci.* **53** (2006) 270, doi:10.1109/TNS.2006.869826.

[64] CMS Collaboration, "Particle–flow event reconstruction in CMS and performance for jets, taus, and $E_{\mathrm{T}}^{\mathrm{miss}}$", CMS Physics Analysis Summary CMS-PAS-PFT-09-001, 2009.

[65] CMS Collaboration, "Commissioning of the particle–flow event reconstruction with the first LHC collisions recorded in the CMS detector", CMS Physics Analysis Summary CMS-PAS-PFT-10-001, 2010.

[66] K. Rose, "Deterministic annealing for clustering, compression, classification, regression and related optimisation problems", *Proceedings of the IEEE* **86** (1998) 2210, doi:10.1109/5.726788.

[67] W. Waltenberger, R. Frühwirth, and P. Vanlaer, "Adaptive vertex fitting", *J. Phys. G* **34** (2007) N343, doi:10.1088/0954-3899/34/12/N01.

[68] CMS Collaboration, "Performance of CMS muon reconstruction in pp collision events at $\sqrt{s} = 7$ TeV", *JINST* **7** (2012) P10002, doi:10.1088/1748-0221/7/10/P10002, arXiv:1206.4071.

[69] H. Voss, A. Höcker, J. Stelzer, and F. Tegenfeldt, "TMVA, the toolkit for multivariate data analysis with ROOT", in *XIth International Workshop on Advanced Computing and Analysis Techniques in Physics Research (ACAT)*, p. 40. 2007. arXiv:physics/0703039.

[70] CMS Collaboration, "Performance of electron reconstruction and selection with the CMS detector in proton-proton collisions at $\sqrt{s} = 8$ TeV", *JINST* **10** (2015) P06005, doi:10.1088/1748-0221/10/06/P06005, arXiv:1502.02701.

[71] M. Cacciari, G. P. Salam, and G. Soyez, "The anti-k_t jet clustering algorithm", *JHEP* **04** (2008) 063, doi:10.1088/1126-6708/2008/04/063, arXiv:0802.1189.

[72] M. Cacciari, G. P. Salam, and G. Soyez, "FastJet user manual", *Eur. Phys. J. C* **72** (2012) 1896, doi:10.1140/epjc/s10052-012-1896-2, arXiv:1111.6097.

[73] M. Cacciari and G. P. Salam, "Dispelling the N^3 myth for the k_t jet-finder", *Phys. Lett. B* **641** (2006) 57, doi:10.1016/j.physletb.2006.08.037, arXiv:hep-ph/0512210.

[74] CMS Collaboration, "Determination of jet energy calibration and transverse momentum resolution in CMS", *JINST* **6** (2011) P11002, doi:10.1088/1748-0221/6/11/P11002, arXiv:1107.4277.

[75] CMS Collaboration, "Identification of b-quark jets with the CMS experiment", *JINST* **8** (2013) P04013, doi:10.1088/1748-0221/8/04/P04013, arXiv:1211.4462.

[76] CMS Collaboration, "Reconstruction and identification of τ lepton decays to hadrons and ν_τ at CMS", *JINST* **11** (2016) P01019, doi:10.1088/1748-0221/11/01/P01019, arXiv:1510.07488.

[77] CMS Collaboration, "Missing transverse energy performance of the CMS detector", *JINST* **6** (2011) P09001, doi:10.1088/1748-0221/6/09/P09001, arXiv:1106.5048.

[78] CMS Collaboration, "Performance of MET reconstruction in CMS", *J. Phys. Conf. Ser.* **587** (2015) 012006, doi:10.1088/1742-6596/587/1/012006.

[79] P. M. Ferreira, J. F. Gunion, H. E. Haber, and R. Santos, "Probing wrong-sign Yukawa couplings at the LHC and a future linear collider", *Phys. Rev. D* **89** (2014) 115003, doi:10.1103/PhysRevD.89.115003, arXiv:1403.4736.

[80] D. Curtin, R. Essig, and Y.-M. Zhong, "Uncovering light scalars with exotic Higgs decays to $b\bar{b}\mu^+\mu^-$", *JHEP* **06** (2015) 025, doi:10.1007/JHEP06(2015)025, arXiv:1412.4779.

[81] LHC Higgs Cross Section Working Group, "Handbook of LHC Higgs cross sections: 1. Inclusive observables", (2011). arXiv:1101.0593.

[82] "NIST Digital library of mathematical functions". http://dlmf.nist.gov , Release 1.0.12 of 2016-09-09.

[83] M. J. Oreglia, "A study of the reactions $\psi' \to \gamma\gamma\psi$". PhD thesis, Stanford University, 1980. SLAC Report SLAC-R-236.

[84] P. D. Dauncey, M. Kenzie, N. Wardle, and G. J. Davies, "Handling uncertainties in background shapes: the discrete profiling method", *JINST* **10** (2015) P04015, doi:10.1088/1748-0221/10/04/P04015, arXiv:1408.6865.

[85] CMS Collaboration, "Observation of the diphoton decay of the Higgs boson and measurement of its properties", *Eur. Phys. J. C* **74** (2014) 3076, doi:10.1140/epjc/s10052-014-3076-z, arXiv:1407.0558.

[86] L. Bianchini, J. Conway, E. K. Friis, and C. Veelken, "Reconstruction of the Higgs mass in H$\to \tau\tau$ events by dynamical likelihood techniques", *J. Phys. Conf. Ser.* **513** (2014) 022035, doi:10.1088/1742-6596/513/2/022035.

[87] J. M. Campbell, R. K. Ellis, and C. Williams, "Vector boson pair production at the LHC", *JHEP* **07** (2011) 018, doi:10.1007/JHEP07(2011)018, arXiv:1105.0020.

[88] CMS Collaboration, "Measurements of inclusive W and Z cross sections in pp collisions at $\sqrt{s} = 7$ TeV", *JHEP* **01** (2011) 080, doi:10.1007/JHEP01(2011)080, arXiv:1012.2466.

[89] S. Alekhin et al., "The PDF4LHC Working Group interim report", (2011). arXiv:1101.0536.

[90] M. Botje et al., "The PDF4LHC Working Group interim recommendations", (2011). arXiv:1101.0538.

[91] CMS Collaboration, "Measurement of the inelastic proton-proton cross section at $\sqrt{s} = 7$ TeV", *Phys. Lett. B* **722** (2013) 5, doi:10.1016/j.physletb.2013.03.024, arXiv:1210.6718.

[92] LHC Higgs Cross Section Working Group, "Handbook of LHC Higgs cross sections: 3. Higgs properties", (2013). arXiv:1307.1347.

[93] LHC Higgs Combination Group, "Procedure for the LHC Higgs boson search combination in Summer 2011", Technical Report CMS-NOTE-2011-005, ATL-PHYS-PUB-2011-11, 2011.

[94] G. Cowan, K. Cranmer, E. Gross, and O. Vitells, "Asymptotic formulae for likelihood-based tests of new physics", *Eur. Phys. J. C* **71** (2011) 1554, doi:10.1140/epjc/s10052-011-1554-0, arXiv:1007.1727. [Erratum: doi:10.1140/epjc/s10052-013-2501-z].

[95] T. Junk, "Confidence level computation for combining searches with small statistics", *Nucl. Instrum. Meth. A* **434** (1999) 435, doi:10.1016/S0168-9002(99)00498-2, arXiv:hep-ex/9902006.

[96] A. L. Read, "Modified frequentist analysis of search results (the CL_s method)", Technical Report CERN-OPEN-2000-005, CERN, 2000.

[97] E. Gross and O. Vitells, "Trial factors or the look elsewhere effect in high energy physics", *Eur. Phys. J. C* **70** (2010) 525, doi:10.1140/epjc/s10052-010-1470-8, arXiv:1005.1891.

A The CMS Collaboration

Yerevan Physics Institute, Yerevan, Armenia
V. Khachatryan, A.M. Sirunyan, A. Tumasyan

Institut für Hochenergiephysik, Wien, Austria
W. Adam, E. Asilar, T. Bergauer, J. Brandstetter, E. Brondolin, M. Dragicevic, J. Erö, M. Flechl, M. Friedl, R. Frühwirth[1], V.M. Ghete, C. Hartl, N. Hörmann, J. Hrubec, M. Jeitler[1], A. König, I. Krätschmer, D. Liko, T. Matsushita, I. Mikulec, D. Rabady, N. Rad, B. Rahbaran, H. Rohringer, J. Schieck[1], J. Strauss, W. Waltenberger, C.-E. Wulz[1]

Institute for Nuclear Problems, Minsk, Belarus
O. Dvornikov, V. Makarenko, V. Zykunov

National Centre for Particle and High Energy Physics, Minsk, Belarus
V. Mossolov, N. Shumeiko, J. Suarez Gonzalez

Universiteit Antwerpen, Antwerpen, Belgium
S. Alderweireldt, E.A. De Wolf, X. Janssen, J. Lauwers, M. Van De Klundert, H. Van Haevermaet, P. Van Mechelen, N. Van Remortel, A. Van Spilbeeck

Vrije Universiteit Brussel, Brussel, Belgium
S. Abu Zeid, F. Blekman, J. D'Hondt, N. Daci, I. De Bruyn, K. Deroover, S. Lowette, S. Moortgat, L. Moreels, A. Olbrechts, Q. Python, S. Tavernier, W. Van Doninck, P. Van Mulders, I. Van Parijs

Université Libre de Bruxelles, Bruxelles, Belgium
H. Brun, B. Clerbaux, G. De Lentdecker, H. Delannoy, G. Fasanella, L. Favart, R. Goldouzian, A. Grebenyuk, G. Karapostoli, T. Lenzi, A. Léonard, J. Luetic, T. Maerschalk, A. Marinov, A. Randle-conde, T. Seva, C. Vander Velde, P. Vanlaer, D. Vannerom, R. Yonamine, F. Zenoni, F. Zhang[2]

Ghent University, Ghent, Belgium
A. Cimmino, T. Cornelis, D. Dobur, A. Fagot, G. Garcia, M. Gul, I. Khvastunov, D. Poyraz, S. Salva, R. Schöfbeck, A. Sharma, M. Tytgat, W. Van Driessche, E. Yazgan, N. Zaganidis

Université Catholique de Louvain, Louvain-la-Neuve, Belgium
H. Bakhshiansohi, C. Beluffi[3], O. Bondu, S. Brochet, G. Bruno, A. Caudron, S. De Visscher, C. Delaere, M. Delcourt, B. Francois, A. Giammanco, A. Jafari, P. Jez, M. Komm, G. Krintiras, V. Lemaitre, A. Magitteri, A. Mertens, M. Musich, C. Nuttens, K. Piotrzkowski, L. Quertenmont, M. Selvaggi, M. Vidal Marono, S. Wertz

Université de Mons, Mons, Belgium
N. Beliy

Centro Brasileiro de Pesquisas Fisicas, Rio de Janeiro, Brazil
W.L. Aldá Júnior, F.L. Alves, G.A. Alves, L. Brito, C. Hensel, A. Moraes, M.E. Pol, P. Rebello Teles

Universidade do Estado do Rio de Janeiro, Rio de Janeiro, Brazil
E. Belchior Batista Das Chagas, W. Carvalho, J. Chinellato[4], A. Custódio, E.M. Da Costa, G.G. Da Silveira[5], D. De Jesus Damiao, C. De Oliveira Martins, S. Fonseca De Souza, L.M. Huertas Guativa, H. Malbouisson, D. Matos Figueiredo, C. Mora Herrera, L. Mundim, H. Nogima, W.L. Prado Da Silva, A. Santoro, A. Sznajder, E.J. Tonelli Manganote[4], A. Vilela Pereira

Universidade Estadual Paulista [a], Universidade Federal do ABC [b], São Paulo, Brazil
S. Ahuja[a], C.A. Bernardes[b], S. Dogra[a], T.R. Fernandez Perez Tomei[a], E.M. Gregores[b], P.G. Mercadante[b], C.S. Moon[a], S.F. Novaes[a], Sandra S. Padula[a], D. Romero Abad[b], J.C. Ruiz Vargas

Institute for Nuclear Research and Nuclear Energy, Sofia, Bulgaria
A. Aleksandrov, R. Hadjiiska, P. Iaydjiev, M. Rodozov, S. Stoykova, G. Sultanov, M. Vutova

University of Sofia, Sofia, Bulgaria
A. Dimitrov, I. Glushkov, L. Litov, B. Pavlov, P. Petkov

Beihang University, Beijing, China
W. Fang[6]

Institute of High Energy Physics, Beijing, China
M. Ahmad, J.G. Bian, G.M. Chen, H.S. Chen, M. Chen, Y. Chen[7], T. Cheng, C.H. Jiang, D. Leggat, Z. Liu, F. Romeo, S.M. Shaheen, A. Spiezia, J. Tao, C. Wang, Z. Wang, H. Zhang, J. Zhao

State Key Laboratory of Nuclear Physics and Technology, Peking University, Beijing, China
Y. Ban, G. Chen, Q. Li, S. Liu, Y. Mao, S.J. Qian, D. Wang, Z. Xu

Universidad de Los Andes, Bogota, Colombia
C. Avila, A. Cabrera, L.F. Chaparro Sierra, C. Florez, J.P. Gomez, C.F. González Hernández, J.D. Ruiz Alvarez, J.C. Sanabria

University of Split, Faculty of Electrical Engineering, Mechanical Engineering and Naval Architecture, Split, Croatia
N. Godinovic, D. Lelas, I. Puljak, P.M. Ribeiro Cipriano, T. Sculac

University of Split, Faculty of Science, Split, Croatia
Z. Antunovic, M. Kovac

Institute Rudjer Boskovic, Zagreb, Croatia
V. Brigljevic, D. Ferencek, K. Kadija, B. Mesic, S. Micanovic, L. Sudic, T. Susa

University of Cyprus, Nicosia, Cyprus
A. Attikis, G. Mavromanolakis, J. Mousa, C. Nicolaou, F. Ptochos, P.A. Razis, H. Rykaczewski, D. Tsiakkouri

Charles University, Prague, Czech Republic
M. Finger[8], M. Finger Jr.[8]

Universidad San Francisco de Quito, Quito, Ecuador
E. Carrera Jarrin

Academy of Scientific Research and Technology of the Arab Republic of Egypt, Egyptian Network of High Energy Physics, Cairo, Egypt
A. Ellithi Kamel[9], M.A. Mahmoud[10,11], A. Radi[11,12]

National Institute of Chemical Physics and Biophysics, Tallinn, Estonia
M. Kadastik, L. Perrini, M. Raidal, A. Tiko, C. Veelken

Department of Physics, University of Helsinki, Helsinki, Finland
P. Eerola, J. Pekkanen, M. Voutilainen

Helsinki Institute of Physics, Helsinki, Finland
J. Härkönen, T. Järvinen, V. Karimäki, R. Kinnunen, T. Lampén, K. Lassila-Perini, S. Lehti, T. Lindén, P. Luukka, J. Tuominiemi, E. Tuovinen, L. Wendland

Lappeenranta University of Technology, Lappeenranta, Finland
J. Talvitie, T. Tuuva

IRFU, CEA, Université Paris-Saclay, Gif-sur-Yvette, France
M. Besancon, F. Couderc, M. Dejardin, D. Denegri, B. Fabbro, J.L. Faure, C. Favaro, F. Ferri, S. Ganjour, S. Ghosh, A. Givernaud, P. Gras, G. Hamel de Monchenault, P. Jarry, I. Kucher, E. Locci, M. Machet, J. Malcles, J. Rander, A. Rosowsky, M. Titov, A. Zghiche

Laboratoire Leprince-Ringuet, Ecole Polytechnique, IN2P3-CNRS, Palaiseau, France
A. Abdulsalam, I. Antropov, S. Baffioni, F. Beaudette, P. Busson, L. Cadamuro, E. Chapon, C. Charlot, O. Davignon, R. Granier de Cassagnac, M. Jo, S. Lisniak, P. Miné, M. Nguyen, C. Ochando, G. Ortona, P. Paganini, P. Pigard, S. Regnard, R. Salerno, Y. Sirois, T. Strebler, Y. Yilmaz, A. Zabi

Institut Pluridisciplinaire Hubert Curien (IPHC), Université de Strasbourg, CNRS-IN2P3
J.-L. Agram[13], J. Andrea, A. Aubin, D. Bloch, J.-M. Brom, M. Buttignol, E.C. Chabert, N. Chanon, C. Collard, E. Conte[13], X. Coubez, J.-C. Fontaine[13], D. Gelé, U. Goerlach, A.-C. Le Bihan, K. Skovpen, P. Van Hove

Centre de Calcul de l'Institut National de Physique Nucleaire et de Physique des Particules, CNRS/IN2P3, Villeurbanne, France
S. Gadrat

Université de Lyon, Université Claude Bernard Lyon 1, CNRS-IN2P3, Institut de Physique Nucléaire de Lyon, Villeurbanne, France
S. Beauceron, C. Bernet, G. Boudoul, E. Bouvier, C.A. Carrillo Montoya, R. Chierici, D. Contardo, B. Courbon, P. Depasse, H. El Mamouni, J. Fan, J. Fay, S. Gascon, M. Gouzevitch, G. Grenier, B. Ille, F. Lagarde, I.B. Laktineh, M. Lethuillier, L. Mirabito, A.L. Pequegnot, S. Perries, A. Popov[14], D. Sabes, V. Sordini, M. Vander Donckt, P. Verdier, S. Viret

Georgian Technical University, Tbilisi, Georgia
T. Toriashvili[15]

Tbilisi State University, Tbilisi, Georgia
Z. Tsamalaidze[8]

RWTH Aachen University, I. Physikalisches Institut, Aachen, Germany
C. Autermann, S. Beranek, L. Feld, A. Heister, M.K. Kiesel, K. Klein, M. Lipinski, A. Ostapchuk, M. Preuten, F. Raupach, S. Schael, C. Schomakers, J. Schulz, T. Verlage, H. Weber

RWTH Aachen University, III. Physikalisches Institut A, Aachen, Germany
A. Albert, M. Brodski, E. Dietz-Laursonn, D. Duchardt, M. Endres, M. Erdmann, S. Erdweg, T. Esch, R. Fischer, A. Güth, M. Hamer, T. Hebbeker, C. Heidemann, K. Hoepfner, S. Knutzen, M. Merschmeyer, A. Meyer, P. Millet, S. Mukherjee, M. Olschewski, K. Padeken, T. Pook, M. Radziej, H. Reithler, M. Rieger, F. Scheuch, L. Sonnenschein, D. Teyssier, S. Thüer

RWTH Aachen University, III. Physikalisches Institut B, Aachen, Germany
V. Cherepanov, G. Flügge, B. Kargoll, T. Kress, A. Künsken, J. Lingemann, T. Müller, A. Nehrkorn, A. Nowack, C. Pistone, O. Pooth, A. Stahl[16]

Deutsches Elektronen-Synchrotron, Hamburg, Germany
M. Aldaya Martin, T. Arndt, C. Asawatangtrakuldee, K. Beernaert, O. Behnke, U. Behrens, A.A. Bin Anuar, K. Borras[17], A. Campbell, P. Connor, C. Contreras-Campana, F. Costanza, C. Diez Pardos, G. Dolinska, G. Eckerlin, D. Eckstein, T. Eichhorn, E. Eren, E. Gallo[18], J. Garay Garcia, A. Geiser, A. Gizhko, J.M. Grados Luyando, P. Gunnellini, A. Harb, J. Hauk, M. Hempel[19], H. Jung, A. Kalogeropoulos, O. Karacheban[19], M. Kasemann, J. Keaveney, C. Kleinwort, I. Korol, D. Krücker, W. Lange, A. Lelek, J. Leonard, K. Lipka, A. Lobanov, W. Lohmann[19], R. Mankel, I.-A. Melzer-Pellmann, A.B. Meyer, G. Mittag, J. Mnich, A. Mussgiller, E. Ntomari, D. Pitzl, R. Placakyte, A. Raspereza, B. Roland, M.Ö. Sahin, P. Saxena, T. Schoerner-Sadenius, C. Seitz, S. Spannagel, N. Stefaniuk, G.P. Van Onsem, R. Walsh, C. Wissing

University of Hamburg, Hamburg, Germany
V. Blobel, M. Centis Vignali, A.R. Draeger, T. Dreyer, E. Garutti, D. Gonzalez, J. Haller, M. Hoffmann, A. Junkes, R. Klanner, R. Kogler, N. Kovalchuk, T. Lapsien, T. Lenz, I. Marchesini, D. Marconi, M. Meyer, M. Niedziela, D. Nowatschin, F. Pantaleo[16], T. Peiffer, A. Perieanu, J. Poehlsen, C. Sander, C. Scharf, P. Schleper, A. Schmidt, S. Schumann, J. Schwandt, H. Stadie, G. Steinbrück, F.M. Stober, M. Stöver, H. Tholen, D. Troendle, E. Usai, L. Vanelderen, A. Vanhoefer, B. Vormwald

Institut für Experimentelle Kernphysik, Karlsruhe, Germany
M. Akbiyik, C. Barth, S. Baur, C. Baus, J. Berger, E. Butz, R. Caspart, T. Chwalek, F. Colombo, W. De Boer, A. Dierlamm, S. Fink, B. Freund, R. Friese, M. Giffels, A. Gilbert, P. Goldenzweig, D. Haitz, F. Hartmann[16], S.M. Heindl, U. Husemann, I. Katkov[14], S. Kudella, H. Mildner, M.U. Mozer, Th. Müller, M. Plagge, G. Quast, K. Rabbertz, S. Röcker, F. Roscher, M. Schröder, I. Shvetsov, G. Sieber, H.J. Simonis, R. Ulrich, S. Wayand, M. Weber, T. Weiler, S. Williamson, C. Wöhrmann, R. Wolf

Institute of Nuclear and Particle Physics (INPP), NCSR Demokritos, Aghia Paraskevi, Greece
G. Anagnostou, G. Daskalakis, T. Geralis, V.A. Giakoumopoulou, A. Kyriakis, D. Loukas, I. Topsis-Giotis

National and Kapodistrian University of Athens, Athens, Greece
S. Kesisoglou, A. Panagiotou, N. Saoulidou, E. Tziaferi

University of Ioánnina, Ioánnina, Greece
I. Evangelou, G. Flouris, C. Foudas, P. Kokkas, N. Loukas, N. Manthos, I. Papadopoulos, E. Paradas

MTA-ELTE Lendület CMS Particle and Nuclear Physics Group, Eötvös Loránd University, Budapest, Hungary
N. Filipovic

Wigner Research Centre for Physics, Budapest, Hungary
G. Bencze, C. Hajdu, D. Horvath[20], F. Sikler, V. Veszpremi, G. Vesztergombi[21], A.J. Zsigmond

Institute of Nuclear Research ATOMKI, Debrecen, Hungary
N. Beni, S. Czellar, J. Karancsi[22], A. Makovec, J. Molnar, Z. Szillasi

Institute of Physics, University of Debrecen
M. Bartók[21], P. Raics, Z.L. Trocsanyi, B. Ujvari

National Institute of Science Education and Research, Bhubaneswar, India
S. Bahinipati, S. Choudhury[23], P. Mal, K. Mandal, A. Nayak[24], D.K. Sahoo, N. Sahoo, S.K. Swain

Panjab University, Chandigarh, India
S. Bansal, S.B. Beri, V. Bhatnagar, R. Chawla, U.Bhawandeep, A.K. Kalsi, A. Kaur, M. Kaur, R. Kumar, P. Kumari, A. Mehta, M. Mittal, J.B. Singh, G. Walia

University of Delhi, Delhi, India
Ashok Kumar, A. Bhardwaj, B.C. Choudhary, R.B. Garg, S. Keshri, S. Malhotra, M. Naimuddin, N. Nishu, K. Ranjan, R. Sharma, V. Sharma

Saha Institute of Nuclear Physics, Kolkata, India
R. Bhattacharya, S. Bhattacharya, K. Chatterjee, S. Dey, S. Dutt, S. Dutta, S. Ghosh, N. Majumdar, A. Modak, K. Mondal, S. Mukhopadhyay, S. Nandan, A. Purohit, A. Roy, D. Roy, S. Roy Chowdhury, S. Sarkar, M. Sharan, S. Thakur

Indian Institute of Technology Madras, Madras, India
P.K. Behera

Bhabha Atomic Research Centre, Mumbai, India
R. Chudasama, D. Dutta, V. Jha, V. Kumar, A.K. Mohanty[16], P.K. Netrakanti, L.M. Pant, P. Shukla, A. Topkar

Tata Institute of Fundamental Research-A, Mumbai, India
T. Aziz, S. Dugad, G. Kole, B. Mahakud, S. Mitra, G.B. Mohanty, B. Parida, N. Sur, B. Sutar

Tata Institute of Fundamental Research-B, Mumbai, India
S. Banerjee, S. Bhowmik[25], R.K. Dewanjee, S. Ganguly, M. Guchait, Sa. Jain, S. Kumar, M. Maity[25], G. Majumder, K. Mazumdar, T. Sarkar[25], N. Wickramage[26]

Indian Institute of Science Education and Research (IISER), Pune, India
S. Chauhan, S. Dube, V. Hegde, A. Kapoor, K. Kothekar, S. Pandey, A. Rane, S. Sharma

Institute for Research in Fundamental Sciences (IPM), Tehran, Iran
S. Chenarani[27], E. Eskandari Tadavani, S.M. Etesami[27], A. Fahim[28], M. Khakzad, M. Mohammadi Najafabadi, M. Naseri, S. Paktinat Mehdiabadi[29], F. Rezaei Hosseinabadi, B. Safarzadeh[30], M. Zeinali

University College Dublin, Dublin, Ireland
M. Felcini, M. Grunewald

INFN Sezione di Bari [a], Università di Bari [b], Politecnico di Bari [c], Bari, Italy
M. Abbrescia[a,b], C. Calabria[a,b], C. Caputo[a,b], A. Colaleo[a], D. Creanza[a,c], L. Cristella[a,b], N. De Filippis[a,c], M. De Palma[a,b], L. Fiore[a], G. Iaselli[a,c], G. Maggi[a,c], M. Maggi[a], G. Miniello[a,b], S. My[a,b], S. Nuzzo[a,b], A. Pompili[a,b], G. Pugliese[a,c], R. Radogna[a,b], A. Ranieri[a], G. Selvaggi[a,b], L. Silvestris[a,16], R. Venditti[a,b], P. Verwilligen[a]

INFN Sezione di Bologna [a], Università di Bologna [b], Bologna, Italy
G. Abbiendi[a], C. Battilana, D. Bonacorsi[a,b], S. Braibant-Giacomelli[a,b], L. Brigliadori[a,b], R. Campanini[a,b], P. Capiluppi[a,b], A. Castro[a,b], F.R. Cavallo[a], S.S. Chhibra[a,b], G. Codispoti[a,b], M. Cuffiani[a,b], G.M. Dallavalle[a], F. Fabbri[a], A. Fanfani[a,b], D. Fasanella[a,b], P. Giacomelli[a], C. Grandi[a], L. Guiducci[a,b], S. Marcellini[a], G. Masetti[a], A. Montanari[a], F.L. Navarria[a,b], A. Perrotta[a], A.M. Rossi[a,b], T. Rovelli[a,b], G.P. Siroli[a,b], N. Tosi[a,b,16]

INFN Sezione di Catania [a], Università di Catania [b], Catania, Italy
S. Albergo[a,b], S. Costa[a,b], A. Di Mattia[a], F. Giordano[a,b], R. Potenza[a,b], A. Tricomi[a,b], C. Tuve[a,b]

INFN Sezione di Firenze [a], Università di Firenze [b], Firenze, Italy
G. Barbagli[a], V. Ciulli[a,b], C. Civinini[a], R. D'Alessandro[a,b], E. Focardi[a,b], P. Lenzi[a,b], M. Meschini[a], S. Paoletti[a], G. Sguazzoni[a], L. Viliani[a,b,16]

INFN Laboratori Nazionali di Frascati, Frascati, Italy
L. Benussi, S. Bianco, F. Fabbri, D. Piccolo, F. Primavera[16]

INFN Sezione di Genova [a], Università di Genova [b], Genova, Italy
V. Calvelli[a,b], F. Ferro[a], M. Lo Vetere[a,b], M.R. Monge[a,b], E. Robutti[a], S. Tosi[a,b]

INFN Sezione di Milano-Bicocca [a], Università di Milano-Bicocca [b], Milano, Italy
L. Brianza[16], M.E. Dinardo[a,b], S. Fiorendi[a,b,16], S. Gennai[a], A. Ghezzi[a,b], P. Govoni[a,b], M. Malberti, S. Malvezzi[a], R.A. Manzoni[a,b,16], D. Menasce[a], L. Moroni[a], M. Paganoni[a,b], D. Pedrini[a], S. Pigazzini, S. Ragazzi[a,b], T. Tabarelli de Fatis[a,b]

INFN Sezione di Napoli [a], Università di Napoli 'Federico II' [b], Napoli, Italy, Università della Basilicata [c], Potenza, Italy, Università G. Marconi [d], Roma, Italy
S. Buontempo[a], N. Cavallo[a,c], G. De Nardo, S. Di Guida[a,d,16], M. Esposito[a,b], F. Fabozzi[a,c], F. Fienga[a,b], A.O.M. Iorio[a,b], G. Lanza[a], L. Lista[a], S. Meola[a,d,16], P. Paolucci[a,16], C. Sciacca[a,b], F. Thyssen

INFN Sezione di Padova [a], Università di Padova [b], Padova, Italy, Università di Trento [c], Trento, Italy
P. Azzi[a,16], N. Bacchetta[a], L. Benato[a,b], D. Bisello[a,b], A. Boletti[a,b], R. Carlin[a,b], A. Carvalho Antunes De Oliveira[a,b], P. Checchia[a], M. Dall'Osso[a,b], P. De Castro Manzano[a], T. Dorigo[a], U. Dosselli[a], F. Gasparini[a,b], U. Gasparini[a,b], A. Gozzelino[a], S. Lacaprara[a], M. Margoni[a,b], A.T. Meneguzzo[a,b], J. Pazzini[a,b], N. Pozzobon[a,b], P. Ronchese[a,b], F. Simonetto[a,b], E. Torassa[a], M. Zanetti, P. Zotto[a,b], G. Zumerle[a,b]

INFN Sezione di Pavia [a], Università di Pavia [b], Pavia, Italy
A. Braghieri[a], A. Magnani[a,b], P. Montagna[a,b], S.P. Ratti[a,b], V. Re[a], C. Riccardi[a,b], P. Salvini[a], I. Vai[a,b], P. Vitulo[a,b]

INFN Sezione di Perugia [a], Università di Perugia [b], Perugia, Italy
L. Alunni Solestizi[a,b], G.M. Bilei[a], D. Ciangottini[a,b], L. Fanò[a,b], P. Lariccia[a,b], R. Leonardi[a,b], G. Mantovani[a,b], M. Menichelli[a], A. Saha[a], A. Santocchia[a,b]

INFN Sezione di Pisa [a], Università di Pisa [b], Scuola Normale Superiore di Pisa [c], Pisa, Italy
K. Androsov[a,31], P. Azzurri[a,16], G. Bagliesi[a], J. Bernardini[a], T. Boccali[a], R. Castaldi[a], M.A. Ciocci[a,31], R. Dell'Orso[a], S. Donato[a,c], G. Fedi, A. Giassi[a], M.T. Grippo[a,31], F. Ligabue[a,c], T. Lomtadze[a], L. Martini[a,b], A. Messineo[a,b], F. Palla[a], A. Rizzi[a,b], A. Savoy-Navarro[a,32], P. Spagnolo[a], R. Tenchini[a], G. Tonelli[a,b], A. Venturi[a], P.G. Verdini[a]

INFN Sezione di Roma [a], Università di Roma [b], Roma, Italy
L. Barone[a,b], F. Cavallari[a], M. Cipriani[a,b], D. Del Re[a,b,16], M. Diemoz[a], S. Gelli[a,b], E. Longo[a,b], F. Margaroli[a,b], B. Marzocchi[a,b], P. Meridiani[a], G. Organtini[a,b], R. Paramatti[a], F. Preiato[a,b], S. Rahatlou[a,b], C. Rovelli[a], F. Santanastasio[a,b]

INFN Sezione di Torino [a], Università di Torino [b], Torino, Italy, Università del Piemonte Orientale [c], Novara, Italy
N. Amapane[a,b], R. Arcidiacono[a,c,16], S. Argiro[a,b], M. Arneodo[a,c], N. Bartosik[a], R. Bellan[a,b], C. Biino[a], N. Cartiglia[a], F. Cenna[a,b], M. Costa[a,b], R. Covarelli[a,b], A. Degano[a,b], N. Demaria[a], L. Finco[a,b], B. Kiani[a,b], C. Mariotti[a], S. Maselli[a], E. Migliore[a,b], V. Monaco[a,b], E. Monteil[a,b], M. Monteno[a], M.M. Obertino[a,b], L. Pacher[a,b], N. Pastrone[a], M. Pelliccioni[a], G.L. Pinna

Angioni[a,b], F. Ravera[a,b], A. Romero[a,b], M. Ruspa[a,c], R. Sacchi[a,b], K. Shchelina[a,b], V. Sola[a], A. Solano[a,b], A. Staiano[a], P. Traczyk[a,b]

INFN Sezione di Trieste [a], Università di Trieste [b], Trieste, Italy
S. Belforte[a], M. Casarsa[a], F. Cossutti[a], G. Della Ricca[a,b], A. Zanetti[a]

Kyungpook National University, Daegu, Korea
D.H. Kim, G.N. Kim, M.S. Kim, S. Lee, S.W. Lee, Y.D. Oh, S. Sekmen, D.C. Son, Y.C. Yang

Chonbuk National University, Jeonju, Korea
A. Lee

Chonnam National University, Institute for Universe and Elementary Particles, Kwangju, Korea
H. Kim

Hanyang University, Seoul, Korea
J.A. Brochero Cifuentes, T.J. Kim

Korea University, Seoul, Korea
S. Cho, S. Choi, Y. Go, D. Gyun, S. Ha, B. Hong, Y. Jo, Y. Kim, B. Lee, K. Lee, K.S. Lee, S. Lee, J. Lim, S.K. Park, Y. Roh

Seoul National University, Seoul, Korea
J. Almond, J. Kim, H. Lee, S.B. Oh, B.C. Radburn-Smith, S.h. Seo, U.K. Yang, H.D. Yoo, G.B. Yu

University of Seoul, Seoul, Korea
M. Choi, H. Kim, J.H. Kim, J.S.H. Lee, I.C. Park, G. Ryu, M.S. Ryu

Sungkyunkwan University, Suwon, Korea
Y. Choi, J. Goh, C. Hwang, J. Lee, I. Yu

Vilnius University, Vilnius, Lithuania
V. Dudenas, A. Juodagalvis, J. Vaitkus

National Centre for Particle Physics, Universiti Malaya, Kuala Lumpur, Malaysia
I. Ahmed, Z.A. Ibrahim, J.R. Komaragiri, M.A.B. Md Ali[33], F. Mohamad Idris[34], W.A.T. Wan Abdullah, M.N. Yusli, Z. Zolkapli

Centro de Investigacion y de Estudios Avanzados del IPN, Mexico City, Mexico
H. Castilla-Valdez, E. De La Cruz-Burelo, I. Heredia-De La Cruz[35], A. Hernandez-Almada, R. Lopez-Fernandez, R. Magaña Villalba, J. Mejia Guisao, A. Sanchez-Hernandez

Universidad Iberoamericana, Mexico City, Mexico
S. Carrillo Moreno, C. Oropeza Barrera, F. Vazquez Valencia

Benemerita Universidad Autonoma de Puebla, Puebla, Mexico
S. Carpinteyro, I. Pedraza, H.A. Salazar Ibarguen, C. Uribe Estrada

Universidad Autónoma de San Luis Potosí, San Luis Potosí, Mexico
A. Morelos Pineda

University of Auckland, Auckland, New Zealand
D. Krofcheck

University of Canterbury, Christchurch, New Zealand
P.H. Butler

National Centre for Physics, Quaid-I-Azam University, Islamabad, Pakistan
A. Ahmad, M. Ahmad, Q. Hassan, H.R. Hoorani, W.A. Khan, A. Saddique, M.A. Shah, M. Shoaib, M. Waqas

National Centre for Nuclear Research, Swierk, Poland
H. Bialkowska, M. Bluj, B. Boimska, T. Frueboes, M. Górski, M. Kazana, K. Nawrocki, K. Romanowska-Rybinska, M. Szleper, P. Zalewski

Institute of Experimental Physics, Faculty of Physics, University of Warsaw, Warsaw, Poland
K. Bunkowski, A. Byszuk[36], K. Doroba, A. Kalinowski, M. Konecki, J. Krolikowski, M. Misiura, M. Olszewski, M. Walczak

Laboratório de Instrumentação e Física Experimental de Partículas, Lisboa, Portugal
P. Bargassa, C. Beirão Da Cruz E Silva, B. Calpas, A. Di Francesco, P. Faccioli, P.G. Ferreira Parracho, M. Gallinaro, J. Hollar, N. Leonardo, L. Lloret Iglesias, M.V. Nemallapudi, J. Rodrigues Antunes, J. Seixas, O. Toldaiev, D. Vadruccio, J. Varela, P. Vischia

Joint Institute for Nuclear Research, Dubna, Russia
S. Afanasiev, P. Bunin, M. Gavrilenko, I. Golutvin, I. Gorbunov, V. Karjavin, A. Lanev, A. Malakhov, V. Matveev[37,38], V. Palichik, V. Perelygin, M. Savina, S. Shmatov, S. Shulha, N. Skatchkov, V. Smirnov, N. Voytishin, A. Zarubin

Petersburg Nuclear Physics Institute, Gatchina (St. Petersburg), Russia
L. Chtchipounov, V. Golovtsov, Y. Ivanov, V. Kim[39], E. Kuznetsova[40], V. Murzin, V. Oreshkin, V. Sulimov, A. Vorobyev

Institute for Nuclear Research, Moscow, Russia
Yu. Andreev, A. Dermenev, S. Gninenko, N. Golubev, A. Karneyeu, M. Kirsanov, N. Krasnikov, A. Pashenkov, D. Tlisov, A. Toropin

Institute for Theoretical and Experimental Physics, Moscow, Russia
V. Epshteyn, V. Gavrilov, N. Lychkovskaya, V. Popov, I. Pozdnyakov, G. Safronov, A. Spiridonov, M. Toms, E. Vlasov, A. Zhokin

Moscow Institute of Physics and Technology, Moscow, Russia
A. Bylinkin[38]

National Research Nuclear University 'Moscow Engineering Physics Institute' (MEPhI), Moscow, Russia
R. Chistov[41], M. Danilov[41], S. Polikarpov

P.N. Lebedev Physical Institute, Moscow, Russia
V. Andreev, M. Azarkin[38], I. Dremin[38], M. Kirakosyan, A. Leonidov[38], A. Terkulov

Skobeltsyn Institute of Nuclear Physics, Lomonosov Moscow State University, Moscow, Russia
A. Baskakov, A. Belyaev, E. Boos, V. Bunichev, M. Dubinin[42], L. Dudko, A. Ershov, A. Gribushin, V. Klyukhin, O. Kodolova, I. Lokhtin, I. Miagkov, S. Obraztsov, S. Petrushanko, V. Savrin

Novosibirsk State University (NSU), Novosibirsk, Russia
V. Blinov[43], Y.Skovpen[43], D. Shtol[43]

State Research Center of Russian Federation, Institute for High Energy Physics, Protvino, Russia
I. Azhgirey, I. Bayshev, S. Bitioukov, D. Elumakhov, V. Kachanov, A. Kalinin, D. Konstantinov, V. Krychkine, V. Petrov, R. Ryutin, A. Sobol, S. Troshin, N. Tyurin, A. Uzunian, A. Volkov

University of Belgrade, Faculty of Physics and Vinca Institute of Nuclear Sciences, Belgrade, Serbia
P. Adzic[44], P. Cirkovic, D. Devetak, M. Dordevic, J. Milosevic, V. Rekovic

Centro de Investigaciones Energéticas Medioambientales y Tecnológicas (CIEMAT), Madrid, Spain
J. Alcaraz Maestre, M. Barrio Luna, E. Calvo, M. Cerrada, M. Chamizo Llatas, N. Colino, B. De La Cruz, A. Delgado Peris, A. Escalante Del Valle, C. Fernandez Bedoya, J.P. Fernández Ramos, J. Flix, M.C. Fouz, P. Garcia-Abia, O. Gonzalez Lopez, S. Goy Lopez, J.M. Hernandez, M.I. Josa, E. Navarro De Martino, A. Pérez-Calero Yzquierdo, J. Puerta Pelayo, A. Quintario Olmeda, I. Redondo, L. Romero, M.S. Soares

Universidad Autónoma de Madrid, Madrid, Spain
J.F. de Trocóniz, M. Missiroli, D. Moran

Universidad de Oviedo, Oviedo, Spain
J. Cuevas, J. Fernandez Menendez, I. Gonzalez Caballero, J.R. González Fernández, E. Palencia Cortezon, S. Sanchez Cruz, I. Suárez Andrés, J.M. Vizan Garcia

Instituto de Física de Cantabria (IFCA), CSIC-Universidad de Cantabria, Santander, Spain
I.J. Cabrillo, A. Calderon, J.R. Castiñeiras De Saa, E. Curras, M. Fernandez, J. Garcia-Ferrero, G. Gomez, A. Lopez Virto, J. Marco, C. Martinez Rivero, F. Matorras, J. Piedra Gomez, T. Rodrigo, A. Ruiz-Jimeno, L. Scodellaro, N. Trevisani, I. Vila, R. Vilar Cortabitarte

CERN, European Organization for Nuclear Research, Geneva, Switzerland
D. Abbaneo, E. Auffray, G. Auzinger, M. Bachtis, P. Baillon, A.H. Ball, D. Barney, P. Bloch, A. Bocci, A. Bonato, C. Botta, T. Camporesi, R. Castello, M. Cepeda, G. Cerminara, M. D'Alfonso, D. d'Enterria, A. Dabrowski, V. Daponte, A. David, M. De Gruttola, A. De Roeck, E. Di Marco[45], M. Dobson, B. Dorney, T. du Pree, D. Duggan, M. Dünser, N. Dupont, A. Elliott-Peisert, S. Fartoukh, G. Franzoni, J. Fulcher, W. Funk, D. Gigi, K. Gill, M. Girone, F. Glege, D. Gulhan, S. Gundacker, M. Guthoff, J. Hammer, P. Harris, J. Hegeman, V. Innocente, P. Janot, J. Kieseler, H. Kirschenmann, V. Knünz, A. Kornmayer[16], M.J. Kortelainen, K. Kousouris, M. Krammer[1], C. Lange, P. Lecoq, C. Lourenço, M.T. Lucchini, L. Malgeri, M. Mannelli, A. Martelli, F. Meijers, J.A. Merlin, S. Mersi, E. Meschi, P. Milenovic[46], F. Moortgat, S. Morovic, M. Mulders, H. Neugebauer, S. Orfanelli, L. Orsini, L. Pape, E. Perez, M. Peruzzi, A. Petrilli, G. Petrucciani, A. Pfeiffer, M. Pierini, A. Racz, T. Reis, G. Rolandi[47], M. Rovere, M. Ruan, H. Sakulin, J.B. Sauvan, C. Schäfer, C. Schwick, M. Seidel, A. Sharma, P. Silva, P. Sphicas[48], J. Steggemann, M. Stoye, Y. Takahashi, M. Tosi, D. Treille, A. Triossi, A. Tsirou, V. Veckalns[49], G.I. Veres[21], M. Verweij, N. Wardle, A. Zagozdzinska[36], W.D. Zeuner

Paul Scherrer Institut, Villigen, Switzerland
W. Bertl, K. Deiters, W. Erdmann, R. Horisberger, Q. Ingram, H.C. Kaestli, D. Kotlinski, U. Langenegger, T. Rohe

Institute for Particle Physics, ETH Zurich, Zurich, Switzerland
F. Bachmair, L. Bäni, L. Bianchini, B. Casal, G. Dissertori, M. Dittmar, M. Donegà, C. Grab, C. Heidegger, D. Hits, J. Hoss, G. Kasieczka, P. Lecomte†, W. Lustermann, B. Mangano, M. Marionneau, P. Martinez Ruiz del Arbol, M. Masciovecchio, M.T. Meinhard, D. Meister, F. Micheli, P. Musella, F. Nessi-Tedaldi, F. Pandolfi, J. Pata, F. Pauss, G. Perrin, L. Perrozzi, M. Quittnat, M. Rossini, M. Schönenberger, A. Starodumov[50], V.R. Tavolaro, K. Theofilatos, R. Wallny

Universität Zürich, Zurich, Switzerland
T.K. Aarrestad, C. Amsler[51], L. Caminada, M.F. Canelli, A. De Cosa, C. Galloni, A. Hinzmann, T. Hreus, B. Kilminster, J. Ngadiuba, D. Pinna, G. Rauco, P. Robmann, D. Salerno, Y. Yang, A. Zucchetta

National Central University, Chung-Li, Taiwan
V. Candelise, T.H. Doan, Sh. Jain, R. Khurana, M. Konyushikhin, C.M. Kuo, W. Lin, Y.J. Lu, A. Pozdnyakov, S.S. Yu

National Taiwan University (NTU), Taipei, Taiwan
Arun Kumar, P. Chang, Y.H. Chang, Y.W. Chang, Y. Chao, K.F. Chen, P.H. Chen, C. Dietz, F. Fiori, W.-S. Hou, Y. Hsiung, Y.F. Liu, R.-S. Lu, M. Miñano Moya, E. Paganis, A. Psallidas, J.f. Tsai, Y.M. Tzeng

Chulalongkorn University, Faculty of Science, Department of Physics, Bangkok, Thailand
B. Asavapibhop, G. Singh, N. Srimanobhas, N. Suwonjandee

Cukurova University - Physics Department, Science and Art Faculty
A. Adiguzel, S. Cerci[52], S. Damarseckin, Z.S. Demiroglu, C. Dozen, I. Dumanoglu, S. Girgis, G. Gokbulut, Y. Guler, I. Hos[53], E.E. Kangal[54], O. Kara, A. Kayis Topaksu, U. Kiminsu, M. Oglakci, G. Onengut[55], K. Ozdemir[56], D. Sunar Cerci[52], H. Topakli[57], S. Turkcapar, I.S. Zorbakir, C. Zorbilmez

Middle East Technical University, Physics Department, Ankara, Turkey
B. Bilin, S. Bilmis, B. Isildak[58], G. Karapinar[59], M. Yalvac, M. Zeyrek

Bogazici University, Istanbul, Turkey
E. Gülmez, M. Kaya[60], O. Kaya[61], E.A. Yetkin[62], T. Yetkin[63]

Istanbul Technical University, Istanbul, Turkey
A. Cakir, K. Cankocak, S. Sen[64]

Institute for Scintillation Materials of National Academy of Science of Ukraine, Kharkov, Ukraine
B. Grynyov

National Scientific Center, Kharkov Institute of Physics and Technology, Kharkov, Ukraine
L. Levchuk, P. Sorokin

University of Bristol, Bristol, United Kingdom
R. Aggleton, F. Ball, L. Beck, J.J. Brooke, D. Burns, E. Clement, D. Cussans, H. Flacher, J. Goldstein, M. Grimes, G.P. Heath, H.F. Heath, J. Jacob, L. Kreczko, C. Lucas, D.M. Newbold[65], S. Paramesvaran, A. Poll, T. Sakuma, S. Seif El Nasr-storey, D. Smith, V.J. Smith

Rutherford Appleton Laboratory, Didcot, United Kingdom
K.W. Bell, A. Belyaev[66], C. Brew, R.M. Brown, L. Calligaris, D. Cieri, D.J.A. Cockerill, J.A. Coughlan, K. Harder, S. Harper, E. Olaiya, D. Petyt, C.H. Shepherd-Themistocleous, A. Thea, I.R. Tomalin, T. Williams

Imperial College, London, United Kingdom
M. Baber, R. Bainbridge, O. Buchmuller, A. Bundock, D. Burton, S. Casasso, M. Citron, D. Colling, L. Corpe, P. Dauncey, G. Davies, A. De Wit, M. Della Negra, R. Di Maria, P. Dunne, A. Elwood, D. Futyan, Y. Haddad, G. Hall, G. Iles, T. James, R. Lane, C. Laner, R. Lucas[65], L. Lyons, A.-M. Magnan, S. Malik, L. Mastrolorenzo, J. Nash, A. Nikitenko[50], J. Pela, B. Penning,

M. Pesaresi, D.M. Raymond, A. Richards, A. Rose, C. Seez, S. Summers, A. Tapper, K. Uchida, M. Vazquez Acosta[67], T. Virdee[16], J. Wright, S.C. Zenz

Brunel University, Uxbridge, United Kingdom
J.E. Cole, P.R. Hobson, A. Khan, P. Kyberd, D. Leslie, I.D. Reid, P. Symonds, L. Teodorescu, M. Turner

Baylor University, Waco, USA
A. Borzou, K. Call, J. Dittmann, K. Hatakeyama, H. Liu, N. Pastika

The University of Alabama, Tuscaloosa, USA
S.I. Cooper, C. Henderson, P. Rumerio, C. West

Boston University, Boston, USA
D. Arcaro, A. Avetisyan, T. Bose, D. Gastler, D. Rankin, C. Richardson, J. Rohlf, L. Sulak, D. Zou

Brown University, Providence, USA
G. Benelli, E. Berry, D. Cutts, A. Garabedian, J. Hakala, U. Heintz, J.M. Hogan, O. Jesus, K.H.M. Kwok, E. Laird, G. Landsberg, Z. Mao, M. Narain, S. Piperov, S. Sagir, E. Spencer, R. Syarif

University of California, Davis, Davis, USA
R. Breedon, G. Breto, D. Burns, M. Calderon De La Barca Sanchez, S. Chauhan, M. Chertok, J. Conway, R. Conway, P.T. Cox, R. Erbacher, C. Flores, G. Funk, M. Gardner, J. Gunion, W. Ko, R. Lander, C. Mclean, M. Mulhearn, D. Pellett, J. Pilot, S. Shalhout, J. Smith, M. Squires, D. Stolp, M. Tripathi

University of California, Los Angeles, USA
C. Bravo, R. Cousins, A. Dasgupta, P. Everaerts, A. Florent, J. Hauser, M. Ignatenko, N. Mccoll, D. Saltzberg, C. Schnaible, E. Takasugi, V. Valuev, M. Weber

University of California, Riverside, Riverside, USA
K. Burt, R. Clare, J. Ellison, J.W. Gary, S.M.A. Ghiasi Shirazi, G. Hanson, J. Heilman, P. Jandir, E. Kennedy, F. Lacroix, O.R. Long, M. Olmedo Negrete, M.I. Paneva, A. Shrinivas, W. Si, H. Wei, S. Wimpenny, B. R. Yates

University of California, San Diego, La Jolla, USA
J.G. Branson, G.B. Cerati, S. Cittolin, M. Derdzinski, R. Gerosa, A. Holzner, D. Klein, V. Krutelyov, J. Letts, I. Macneill, D. Olivito, S. Padhi, M. Pieri, M. Sani, V. Sharma, S. Simon, M. Tadel, A. Vartak, S. Wasserbaech[68], C. Welke, J. Wood, F. Würthwein, A. Yagil, G. Zevi Della Porta

University of California, Santa Barbara - Department of Physics, Santa Barbara, USA
N. Amin, R. Bhandari, J. Bradmiller-Feld, C. Campagnari, A. Dishaw, V. Dutta, M. Franco Sevilla, C. George, F. Golf, L. Gouskos, J. Gran, R. Heller, J. Incandela, S.D. Mullin, A. Ovcharova, H. Qu, J. Richman, D. Stuart, I. Suarez, J. Yoo

California Institute of Technology, Pasadena, USA
D. Anderson, A. Apresyan, J. Bendavid, A. Bornheim, J. Bunn, Y. Chen, J. Duarte, J.M. Lawhorn, A. Mott, H.B. Newman, C. Pena, M. Spiropulu, J.R. Vlimant, S. Xie, R.Y. Zhu

Carnegie Mellon University, Pittsburgh, USA
M.B. Andrews, V. Azzolini, T. Ferguson, M. Paulini, J. Russ, M. Sun, H. Vogel, I. Vorobiev, M. Weinberg

University of Colorado Boulder, Boulder, USA
J.P. Cumalat, W.T. Ford, F. Jensen, A. Johnson, M. Krohn, T. Mulholland, K. Stenson, S.R. Wagner

Cornell University, Ithaca, USA
J. Alexander, J. Chaves, J. Chu, S. Dittmer, K. Mcdermott, N. Mirman, G. Nicolas Kaufman, J.R. Patterson, A. Rinkevicius, A. Ryd, L. Skinnari, L. Soffi, S.M. Tan, Z. Tao, J. Thom, J. Tucker, P. Wittich, M. Zientek

Fairfield University, Fairfield, USA
D. Winn

Fermi National Accelerator Laboratory, Batavia, USA
S. Abdullin, M. Albrow, G. Apollinari, S. Banerjee, L.A.T. Bauerdick, A. Beretvas, J. Berryhill, P.C. Bhat, G. Bolla, K. Burkett, J.N. Butler, H.W.K. Cheung, F. Chlebana, S. Cihangir†, M. Cremonesi, V.D. Elvira, I. Fisk, J. Freeman, E. Gottschalk, L. Gray, D. Green, S. Grünendahl, O. Gutsche, D. Hare, R.M. Harris, S. Hasegawa, J. Hirschauer, Z. Hu, B. Jayatilaka, S. Jindariani, M. Johnson, U. Joshi, B. Klima, B. Kreis, S. Lammel, J. Linacre, D. Lincoln, R. Lipton, T. Liu, R. Lopes De Sá, J. Lykken, K. Maeshima, N. Magini, J.M. Marraffino, S. Maruyama, D. Mason, P. McBride, P. Merkel, S. Mrenna, S. Nahn, V. O'Dell, K. Pedro, O. Prokofyev, G. Rakness, L. Ristori, E. Sexton-Kennedy, A. Soha, W.J. Spalding, L. Spiegel, S. Stoynev, N. Strobbe, L. Taylor, S. Tkaczyk, N.V. Tran, L. Uplegger, E.W. Vaandering, C. Vernieri, M. Verzocchi, R. Vidal, M. Wang, H.A. Weber, A. Whitbeck, Y. Wu

University of Florida, Gainesville, USA
D. Acosta, P. Avery, P. Bortignon, D. Bourilkov, A. Brinkerhoff, A. Carnes, M. Carver, D. Curry, S. Das, R.D. Field, I.K. Furic, J. Konigsberg, A. Korytov, J.F. Low, P. Ma, K. Matchev, H. Mei, G. Mitselmakher, D. Rank, L. Shchutska, D. Sperka, L. Thomas, J. Wang, S. Wang, J. Yelton

Florida International University, Miami, USA
S. Linn, P. Markowitz, G. Martinez, J.L. Rodriguez

Florida State University, Tallahassee, USA
A. Ackert, J.R. Adams, T. Adams, A. Askew, S. Bein, B. Diamond, S. Hagopian, V. Hagopian, K.F. Johnson, H. Prosper, A. Santra, R. Yohay

Florida Institute of Technology, Melbourne, USA
M.M. Baarmand, V. Bhopatkar, S. Colafranceschi, M. Hohlmann, D. Noonan, T. Roy, F. Yumiceva

University of Illinois at Chicago (UIC), Chicago, USA
M.R. Adams, L. Apanasevich, D. Berry, R.R. Betts, I. Bucinskaite, R. Cavanaugh, O. Evdokimov, L. Gauthier, C.E. Gerber, D.J. Hofman, K. Jung, P. Kurt, C. O'Brien, I.D. Sandoval Gonzalez, P. Turner, N. Varelas, H. Wang, Z. Wu, M. Zakaria, J. Zhang

The University of Iowa, Iowa City, USA
B. Bilki[69], W. Clarida, K. Dilsiz, S. Durgut, R.P. Gandrajula, M. Haytmyradov, V. Khristenko, J.-P. Merlo, H. Mermerkaya[70], A. Mestvirishvili, A. Moeller, J. Nachtman, H. Ogul, Y. Onel, F. Ozok[71], A. Penzo, C. Snyder, E. Tiras, J. Wetzel, K. Yi

Johns Hopkins University, Baltimore, USA
I. Anderson, B. Blumenfeld, A. Cocoros, N. Eminizer, D. Fehling, L. Feng, A.V. Gritsan, P. Maksimovic, C. Martin, M. Osherson, J. Roskes, U. Sarica, M. Swartz, M. Xiao, Y. Xin, C. You

The University of Kansas, Lawrence, USA
A. Al-bataineh, P. Baringer, A. Bean, S. Boren, J. Bowen, C. Bruner, J. Castle, L. Forthomme, R.P. Kenny III, S. Khalil, A. Kropivnitskaya, D. Majumder, W. Mcbrayer, M. Murray, S. Sanders, R. Stringer, J.D. Tapia Takaki, Q. Wang

Kansas State University, Manhattan, USA
A. Ivanov, K. Kaadze, Y. Maravin, A. Mohammadi, L.K. Saini, N. Skhirtladze, S. Toda

Lawrence Livermore National Laboratory, Livermore, USA
F. Rebassoo, D. Wright

University of Maryland, College Park, USA
C. Anelli, A. Baden, O. Baron, A. Belloni, B. Calvert, S.C. Eno, C. Ferraioli, J.A. Gomez, N.J. Hadley, S. Jabeen, R.G. Kellogg, T. Kolberg, J. Kunkle, Y. Lu, A.C. Mignerey, F. Ricci-Tam, Y.H. Shin, A. Skuja, M.B. Tonjes, S.C. Tonwar

Massachusetts Institute of Technology, Cambridge, USA
D. Abercrombie, B. Allen, A. Apyan, R. Barbieri, A. Baty, R. Bi, K. Bierwagen, S. Brandt, W. Busza, I.A. Cali, Z. Demiragli, L. Di Matteo, G. Gomez Ceballos, M. Goncharov, D. Hsu, Y. Iiyama, G.M. Innocenti, M. Klute, D. Kovalskyi, K. Krajczar, Y.S. Lai, Y.-J. Lee, A. Levin, P.D. Luckey, B. Maier, A.C. Marini, C. Mcginn, C. Mironov, S. Narayanan, X. Niu, C. Paus, C. Roland, G. Roland, J. Salfeld-Nebgen, G.S.F. Stephans, K. Sumorok, K. Tatar, M. Varma, D. Velicanu, J. Veverka, J. Wang, T.W. Wang, B. Wyslouch, M. Yang, V. Zhukova

University of Minnesota, Minneapolis, USA
A.C. Benvenuti, R.M. Chatterjee, A. Evans, A. Finkel, A. Gude, P. Hansen, S. Kalafut, S.C. Kao, Y. Kubota, Z. Lesko, J. Mans, S. Nourbakhsh, N. Ruckstuhl, R. Rusack, N. Tambe, J. Turkewitz

University of Mississippi, Oxford, USA
J.G. Acosta, S. Oliveros

University of Nebraska-Lincoln, Lincoln, USA
E. Avdeeva, R. Bartek[72], K. Bloom, D.R. Claes, A. Dominguez[72], C. Fangmeier, R. Gonzalez Suarez, R. Kamalieddin, I. Kravchenko, A. Malta Rodrigues, F. Meier, J. Monroy, J.E. Siado, G.R. Snow, B. Stieger

State University of New York at Buffalo, Buffalo, USA
M. Alyari, J. Dolen, J. George, A. Godshalk, C. Harrington, I. Iashvili, J. Kaisen, A. Kharchilava, A. Kumar, A. Parker, S. Rappoccio, B. Roozbahani

Northeastern University, Boston, USA
G. Alverson, E. Barberis, A. Hortiangtham, A. Massironi, D.M. Morse, D. Nash, T. Orimoto, R. Teixeira De Lima, D. Trocino, R.-J. Wang, D. Wood

Northwestern University, Evanston, USA
S. Bhattacharya, O. Charaf, K.A. Hahn, A. Kubik, A. Kumar, N. Mucia, N. Odell, B. Pollack, M.H. Schmitt, K. Sung, M. Trovato, M. Velasco

University of Notre Dame, Notre Dame, USA
N. Dev, M. Hildreth, K. Hurtado Anampa, C. Jessop, D.J. Karmgard, N. Kellams, K. Lannon, N. Marinelli, F. Meng, C. Mueller, Y. Musienko[37], M. Planer, A. Reinsvold, R. Ruchti, G. Smith, S. Taroni, M. Wayne, M. Wolf, A. Woodard

The Ohio State University, Columbus, USA
J. Alimena, L. Antonelli, B. Bylsma, L.S. Durkin, S. Flowers, B. Francis, A. Hart, C. Hill, R. Hughes, W. Ji, B. Liu, W. Luo, D. Puigh, B.L. Winer, H.W. Wulsin

Princeton University, Princeton, USA
S. Cooperstein, O. Driga, P. Elmer, J. Hardenbrook, P. Hebda, D. Lange, J. Luo, D. Marlow, J. Mc Donald, T. Medvedeva, K. Mei, M. Mooney, J. Olsen, C. Palmer, P. Piroué, D. Stickland, A. Svyatkovskiy, C. Tully, A. Zuranski

University of Puerto Rico, Mayaguez, USA
S. Malik

Purdue University, West Lafayette, USA
A. Barker, V.E. Barnes, S. Folgueras, L. Gutay, M.K. Jha, M. Jones, A.W. Jung, A. Khatiwada, D.H. Miller, N. Neumeister, J.F. Schulte, X. Shi, J. Sun, F. Wang, W. Xie

Purdue University Calumet, Hammond, USA
N. Parashar, J. Stupak

Rice University, Houston, USA
A. Adair, B. Akgun, Z. Chen, K.M. Ecklund, F.J.M. Geurts, M. Guilbaud, W. Li, B. Michlin, M. Northup, B.P. Padley, R. Redjimi, J. Roberts, J. Rorie, Z. Tu, J. Zabel

University of Rochester, Rochester, USA
B. Betchart, A. Bodek, P. de Barbaro, R. Demina, Y.t. Duh, T. Ferbel, M. Galanti, A. Garcia-Bellido, J. Han, O. Hindrichs, A. Khukhunaishvili, K.H. Lo, P. Tan, M. Verzetti

Rutgers, The State University of New Jersey, Piscataway, USA
A. Agapitos, J.P. Chou, E. Contreras-Campana, Y. Gershtein, T.A. Gómez Espinosa, E. Halkiadakis, M. Heindl, D. Hidas, E. Hughes, S. Kaplan, R. Kunnawalkam Elayavalli, S. Kyriacou, A. Lath, K. Nash, H. Saka, S. Salur, S. Schnetzer, D. Sheffield, S. Somalwar, R. Stone, S. Thomas, P. Thomassen, M. Walker

University of Tennessee, Knoxville, USA
A.G. Delannoy, M. Foerster, J. Heideman, G. Riley, K. Rose, S. Spanier, K. Thapa

Texas A&M University, College Station, USA
O. Bouhali[73], A. Celik, M. Dalchenko, M. De Mattia, A. Delgado, S. Dildick, R. Eusebi, J. Gilmore, T. Huang, E. Juska, T. Kamon[74], R. Mueller, Y. Pakhotin, R. Patel, A. Perloff, L. Perniè, D. Rathjens, A. Rose, A. Safonov, A. Tatarinov, K.A. Ulmer

Texas Tech University, Lubbock, USA
N. Akchurin, C. Cowden, J. Damgov, F. De Guio, C. Dragoiu, P.R. Dudero, J. Faulkner, E. Gurpinar, S. Kunori, K. Lamichhane, S.W. Lee, T. Libeiro, T. Peltola, S. Undleeb, I. Volobouev, Z. Wang

Vanderbilt University, Nashville, USA
S. Greene, A. Gurrola, R. Janjam, W. Johns, C. Maguire, A. Melo, H. Ni, P. Sheldon, S. Tuo, J. Velkovska, Q. Xu

University of Virginia, Charlottesville, USA
M.W. Arenton, P. Barria, B. Cox, J. Goodell, R. Hirosky, A. Ledovskoy, H. Li, C. Neu, T. Sinthuprasith, X. Sun, Y. Wang, E. Wolfe, F. Xia

Wayne State University, Detroit, USA
C. Clarke, R. Harr, P.E. Karchin, J. Sturdy

University of Wisconsin - Madison, Madison, WI, USA
D.A. Belknap, J. Buchanan, C. Caillol, S. Dasu, L. Dodd, S. Duric, B. Gomber, M. Grothe, M. Herndon, A. Hervé, P. Klabbers, A. Lanaro, A. Levine, K. Long, R. Loveless, I. Ojalvo, T. Perry, G.A. Pierro, G. Polese, T. Ruggles, A. Savin, N. Smith, W.H. Smith, D. Taylor, N. Woods

†: Deceased
1: Also at Vienna University of Technology, Vienna, Austria
2: Also at State Key Laboratory of Nuclear Physics and Technology, Peking University, Beijing, China
3: Also at Institut Pluridisciplinaire Hubert Curien (IPHC), Université de Strasbourg, CNRS/IN2P3, Strasbourg, France
4: Also at Universidade Estadual de Campinas, Campinas, Brazil
5: Also at Universidade Federal de Pelotas, Pelotas, Brazil
6: Also at Université Libre de Bruxelles, Bruxelles, Belgium
7: Also at Deutsches Elektronen-Synchrotron, Hamburg, Germany
8: Also at Joint Institute for Nuclear Research, Dubna, Russia
9: Now at Cairo University, Cairo, Egypt
10: Also at Fayoum University, El-Fayoum, Egypt
11: Now at British University in Egypt, Cairo, Egypt
12: Now at Ain Shams University, Cairo, Egypt
13: Also at Université de Haute Alsace, Mulhouse, France
14: Also at Skobeltsyn Institute of Nuclear Physics, Lomonosov Moscow State University, Moscow, Russia
15: Also at Tbilisi State University, Tbilisi, Georgia
16: Also at CERN, European Organization for Nuclear Research, Geneva, Switzerland
17: Also at RWTH Aachen University, III. Physikalisches Institut A, Aachen, Germany
18: Also at University of Hamburg, Hamburg, Germany
19: Also at Brandenburg University of Technology, Cottbus, Germany
20: Also at Institute of Nuclear Research ATOMKI, Debrecen, Hungary
21: Also at MTA-ELTE Lendület CMS Particle and Nuclear Physics Group, Eötvös Loránd University, Budapest, Hungary
22: Also at Institute of Physics, University of Debrecen, Debrecen, Hungary
23: Also at Indian Institute of Science Education and Research, Bhopal, India
24: Also at Institute of Physics, Bhubaneswar, India
25: Also at University of Visva-Bharati, Santiniketan, India
26: Also at University of Ruhuna, Matara, Sri Lanka
27: Also at Isfahan University of Technology, Isfahan, Iran
28: Also at University of Tehran, Department of Engineering Science, Tehran, Iran
29: Also at Yazd University, Yazd, Iran
30: Also at Plasma Physics Research Center, Science and Research Branch, Islamic Azad University, Tehran, Iran
31: Also at Università degli Studi di Siena, Siena, Italy
32: Also at Purdue University, West Lafayette, USA
33: Also at International Islamic University of Malaysia, Kuala Lumpur, Malaysia
34: Also at Malaysian Nuclear Agency, MOSTI, Kajang, Malaysia
35: Also at Consejo Nacional de Ciencia y Tecnología, Mexico city, Mexico
36: Also at Warsaw University of Technology, Institute of Electronic Systems, Warsaw, Poland
37: Also at Institute for Nuclear Research, Moscow, Russia
38: Now at National Research Nuclear University 'Moscow Engineering Physics Institute' (MEPhI), Moscow, Russia

39: Also at St. Petersburg State Polytechnical University, St. Petersburg, Russia
40: Also at University of Florida, Gainesville, USA
41: Also at P.N. Lebedev Physical Institute, Moscow, Russia
42: Also at California Institute of Technology, Pasadena, USA
43: Also at Budker Institute of Nuclear Physics, Novosibirsk, Russia
44: Also at Faculty of Physics, University of Belgrade, Belgrade, Serbia
45: Also at INFN Sezione di Roma; Università di Roma, Roma, Italy
46: Also at University of Belgrade, Faculty of Physics and Vinca Institute of Nuclear Sciences, Belgrade, Serbia
47: Also at Scuola Normale e Sezione dell'INFN, Pisa, Italy
48: Also at National and Kapodistrian University of Athens, Athens, Greece
49: Also at Riga Technical University, Riga, Latvia
50: Also at Institute for Theoretical and Experimental Physics, Moscow, Russia
51: Also at Albert Einstein Center for Fundamental Physics, Bern, Switzerland
52: Also at Adiyaman University, Adiyaman, Turkey
53: Also at Istanbul Aydin University, Istanbul, Turkey
54: Also at Mersin University, Mersin, Turkey
55: Also at Cag University, Mersin, Turkey
56: Also at Piri Reis University, Istanbul, Turkey
57: Also at Gaziosmanpasa University, Tokat, Turkey
58: Also at Ozyegin University, Istanbul, Turkey
59: Also at Izmir Institute of Technology, Izmir, Turkey
60: Also at Marmara University, Istanbul, Turkey
61: Also at Kafkas University, Kars, Turkey
62: Also at Istanbul Bilgi University, Istanbul, Turkey
63: Also at Yildiz Technical University, Istanbul, Turkey
64: Also at Hacettepe University, Ankara, Turkey
65: Also at Rutherford Appleton Laboratory, Didcot, United Kingdom
66: Also at School of Physics and Astronomy, University of Southampton, Southampton, United Kingdom
67: Also at Instituto de Astrofísica de Canarias, La Laguna, Spain
68: Also at Utah Valley University, Orem, USA
69: Also at Argonne National Laboratory, Argonne, USA
70: Also at Erzincan University, Erzincan, Turkey
71: Also at Mimar Sinan University, Istanbul, Istanbul, Turkey
72: Now at The Catholic University of America, Washington, USA
73: Also at Texas A&M University at Qatar, Doha, Qatar
74: Also at Kyungpook National University, Daegu, Korea